INSTITUTE OF TECHNOLOGY

AIR UNIVERSITY

UNITED STATES AIR FORCE

SCHOOL OF ENGINEERING

THESIS

WRIGHT-PATTERSON AIR FORCE BASE, OHIO

AF-WP-B-SEP 60 5M

THEORETICAL ANALYSIS OF A CYLINDRICAL FAST REACTOR CONTAINING CONCENTRIC ANNULAR VOIDS

THESIS

Presented to the Faculty of the School of Engineering

of the Institute of Technology

Air University

in Partial Fulfillment of the

Requirement for the Degree of

Master of Science

By

James H. Mann

Captain U.S.A.F.

Graduate Nuclear Engineering

March 1961

Erratta

The ratio H/D shown on page 46 should be D/H $\approx$ 1.1, to give a minimum volume for the cylindrical core.

Preface

The purpose of this thesis is to provide the first engineering estimates of a fast, pulse-type reactor. There is no attempt made to justify the construction of such a reactor. However, as the report indicates, a configuration consisting of a layered structure of thin-walled concentric cylinders composed of highly enriched uranium and 10% by weight molybdenum does offer better performance capabilities than that offered by existing facilities. The layered structure tends to reduce the mechanical stresses and thermal shock caused by a pulsing action and the addition of molybdenum to uranium improves the high temperature properties of the fuel elements.

In this discussion, certain liberties are taken in regards to the technical level of the reader. Primarily, it was assumed that the reader is familiar with the established techniques of converting heat energy into mechanical energy and the conversion of microscopic cross sections into macroscopic cross sections. If the reader is not familiar with these techniques, they may be found in any good reactor technology text book. In addition, the sample calculations in Appendix B contain only supplementary information relative to the Multigroup Asymptotic Iteration Method used to derive the material buckling of the system. It was felt that all other calculations were sufficiently detailed in the body of the

report and that any attempt to further clarify them would be superfluous. For the convenience of the reader, Appendix A contains a complete glossary of all the symbols used in this report.

The author wishes to express his gratitude to Major James R. Bohannon, of the Institute of Technology Physics Department, for his patience and invaluable technical guidance without which this report would have never been possible. In addition, thanks is expressed to First Lieutenant L.R. McCulloh, of the Mathematics Department, for his assistance in clarifying several of the mathematical theories involved in this analysis. Gratitude and sympathy is extended to the author's wife, Pollyanna, for her many hours spent typing and re-typing this report.

James H. Mann

Contents

List of Figures

List of Tables

Abstract

This report contains the first engineering estimates for a proposed fast, pulse-type reactor. The reactor consists of a layered structure of thin-walled concentric cylinders composed of uranium and 10% by weight molybdenum.

Design requirements and the advantages of the proposed design over existing facilities are discussed. The Multigroup Asymptotic Transport Method is used to determine the material buckling and clean-cold critical mass of a solid, bare, cylindrical cylinder, which serves as a base for the proposed design. Based on the maximum thermal expansion that occurs throughout the operating temperature ranges, the optimum size of the shells and coolant channel voids is determined.

A central channel, to provide a means for pulsing the assembly, and the annular cooling voids were introduced into the core and the effects of same are analyzed. Then, a new critical mass is computed.

Performance characteristics during a pulsing cycle are computed, based on the maximum allowable temperature rise, and compared to the performance of Godiva II. In all cases, the proposed facility indicates a decided improvement over the existing prototypes in its operating capabilities.

The results of this analysis appears to indicate that the proposed design is feasible in addition to advancing the "state of the art" as it exists in pulsing facilities. However, further analysis is needed and recommendations for these future investigations are contained in the conclusion of this report.

THEORETICAL ANALYSIS OF A CYLINDRICAL FAST REACTOR CONTAINING CONCENTRIC ANNULAR VOIDS

I. Introduction

The purpose of this report is to provide a first engineering estimate of the parameters involved in the design of a fast, pulse-type reactor. No attempt will be made to justify the reactor, but the justification for the design will be covered. The proposed design consists of a layered structure of thin-walled concentric cylinders composed of highly enriched uranium and 10%, by weight, of molybdenum (Fig. 1). Before going into the particulars of the analysis, a discussion of the history, uses, and the method of analysis is given in the following paragraphs.

Prototypes

Previous experience with pulsing reactors has been limited to experiments conducted with the two Godiva assemblies. Godiva I was a bare, spherical, uranium metal critical assembly that produced a total of approximately 1000 bursts before its retirement following an accidentally intense burst (Ref. 34).

The Godiva II is also composed of bare uranium metal in the form of a solid right circular cylinder with a spherically shaped top

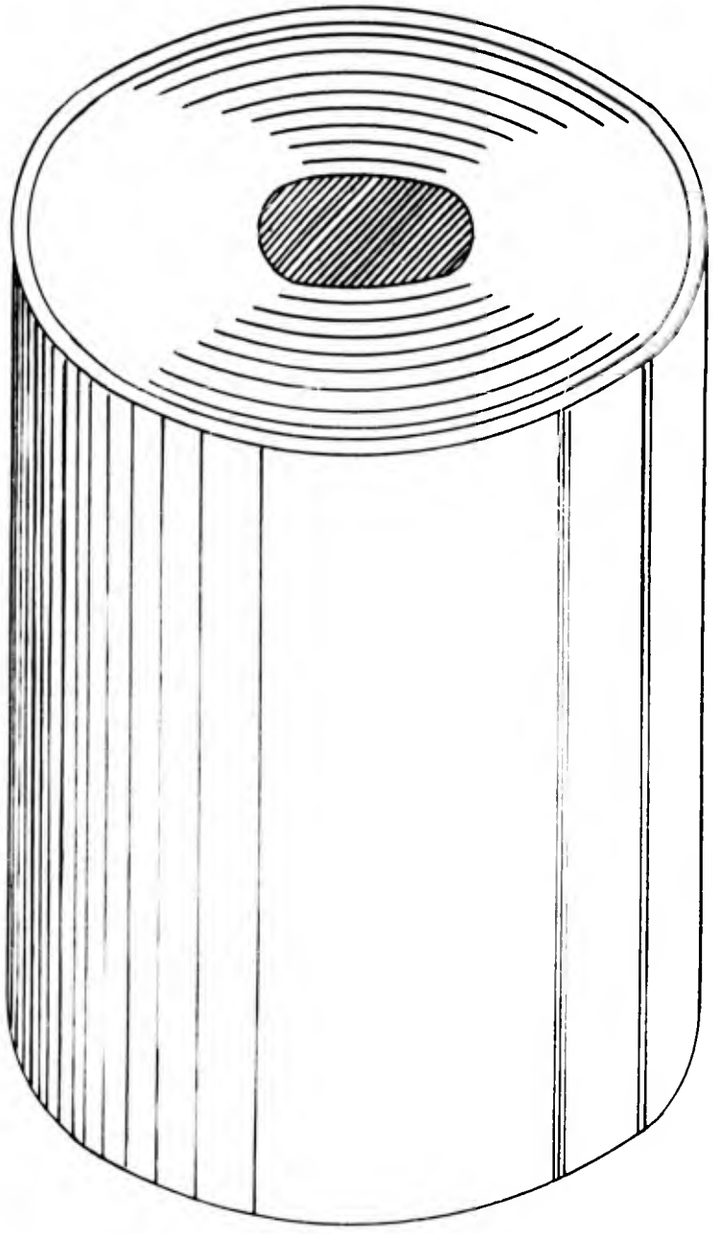

Figure 1

Pulse Facility Core

(Ref. 33). Although these reactors were invaluable in early neutron pulse irradiation investigations, they did have their shortcomings. Specifically, both reactors had low heat capacities, low resistance to thermal shock, limited daily cyclic operation, and finally, as a result of the previously mentioned properties, they were limited in the available leakage flux, peak flux, and short pulse duration (Ref. 33). Consequently, the desired level of performance was never quite achieved with these reactors, i.e., there was always a lack of experimental space around the reactor because of the limited cyclic operation and, in addition, the leakage spectra did not simulate the weapons burst spectra, in either energy or neutron flux, as well as desired. In both cases, these limitations were caused by the restrictions imposed on the system by the maximum allowable temperature rise.

The Godiva II reactor is limited to a temperature rise of about 100° C at the hottest point in the pulse mode of operation and, therefore, to a total yield of about 10^{16} fissions. This limitation is imposed because of the thermal stresses and the resultant mechanical shock which occur in the large uranium metal blocks which compose the assembly after a sudden rise in temperature. Furthermore, the thermal stresses also retard the shut-down mechanism which is the thermal expansion. This effect, already manifest at 10^{16} fissions, enhances the yield and thus is a potential hazard. These

limitations were also applicable to the Godiva I prior to its retirement.

Potential Utilizations

There are many specific utilizations for which a pulse reactor is particularly adaptable. For instance, in the past, the neutronic effects in critical assemblies following a rapid insertion of excess reactivity were studied by the use of a particle accelerator to generate the neutrons. The pulse time widths thereby achieved were quite satisfactory, but the neutron flux intensities were far inferior to that which could be attained with a fast, pulse-type reactor.

In radiation damage studies investigating the effects on the components of various systems, difficulties were encountered because much of the radiation annealed out at operating temperatures. With this facility, the radiation damage could be produced at a rate that would be much shorter than the annealing times of the components. Thus, radiation damage studies can be conducted which are impossible with existing techniques.

Another field of current interest is the neutron pulse irradiation effect on materials. Of prime interest is the effect on semiconductors. The effect of photon and fast particle irradiation on the electrical properties of semi-conductor devices can be sufficient to seriously impair or totally destroy the ability of these devices

to operate. Steady state radiation studies cannot be employed to predict transient or dose rate effects, energy effects, or annealing effects. The carrier concentration and the carrier lifetime changes in germanium, silicon and certain intermetallic compounds are of particular interest. As few as 10^{10} fast neutrons/cm^2 produce measurable changes in the number of recombination centers in germanium (Ref. 34). A pulsing facility can provide a flux of this magnitude and is therefore adequate to produce radiation damage effects of this type. In addition to semi-conductor materials, the frequency shift and the changes in the constants of peizo-electric crystals caused by irradiation can be investigated using these techniques. Physical and solid state properties of many materials are affected by high dose rate irradiation, consequently, pulsing techniques are of manifest interest in these particular applications.

Method of Analysis

The theoretical analysis of a reactor normally requires investigations relative to the clean-cold critical mass, physical dimensions, leakage, time response, and finally, in this specific instance, optimization of the layered dimensions. However, prior to these investigations, it is first necessary to establish the exact requirements of the system. Consequently, Section II is devoted to the establishment of these design criteria.

After the design requirements are established, the advantages

offered by the proposed configuration and composition are discussed in Section III. This discussion includes the justification for the proposed design.

The major efforts expended in the analysis is presented in the subsequent sections. There are several methods that might have been suitable for this analysis, however, for the purposes of this study the following procedure was used:

1. The Multigroup Asymptotic Transport Iteration Method was used to determine the material buckling of a critical system composed of uranium and 10% by weight of molybdenum (Ref. 21).

2. Material buckling was then equated to the geometric buckling of a solid, right-circular cylinder, of the same composition, and the dimensions and clean-cold critical mass was computed.

3. Based on the maximum thermal expansion that occurs throughout the operating temperature ranges, the dimensions of the voids were determined.

4. By introducing new boundary conditions to the solution of the neutron diffusion equation for the flux distribution in a cylinder, the effects of introducing a central void and annular voids in the system were established and a new critical mass was calculated (Ref. 12).

5. Physical dimensions of the shells were arbitrarily selected on the basis of empirical data collected relative to short

heat transfer path and structural integrity, i.e., tensile strength, yield strength, hardness, etc. (Ref. 30).

6. A relative flux was computed for various positions in the core and a flux plot was constructed.

7. The total energy expended in a pulse was computed based on the maximum allowable temperature rise in the U-10 w/o Mo alloy.

8. From the total energy expended, the total yield was determined based on the performance of Godiva II (Ref. 34).

9. Total leakage and surface leakage was computed based on the total yield, and determined by using characteristic values also from Godiva II.

10. Finally, the peak power was computed assuming a pulse width of 10 μ seconds (Ref. 19).

II. Design Requirements

The primary objective of a pulse reactor is to simulate the radiation environment associated with nuclear weapon bursts. In order to accomplish this, as well as to allow variation for rate effect thresholds, the reactor must feature a pure source of reasonably energetic neutrons, a pulse width variable down to a few microseconds, and a large dose per pulse.

Nuclear Weapon Neutron Spectrum

It is important in connection with the measurement of nuclear bomb neutrons and the study of their effects to know something of the manner in which the distribution of neutron energies varies with distance from the explosion. From a series of measurements made at the nuclear test explosions in Nevada in 1955, it seems that, at least for the devices tested, the energy spectrum remains the same for a given device over the range of distances which are of primary interest (Ref. 14).

The probable explanation of this important result is that, due to a combination of circumstances, the loss of thermal neutrons by capture is just compensated by the slowing down of fast neutrons. The total number of neutrons received per unit area at a given location is less the farther that point is from the explosion, because, in addition to being spread over a large area, some of the

faster neutrons are slowed down and the slower ones are removed by capture. But the proportion or fraction of neutrons in any particular energy range appears to be essentially the same at all distances of interest. Therefore, the total dose and dose rate at any given point is just a function of the distance from the explosion and the design of the weapon.

Neutron Leakage

From a consideration of the above factors, the leakage at the surface of the pulse reactor should have an energy spectrum that closely approximates the fast fission spectrum itself. This assumes that the standard fission neutron energy spectrum is representative of the fission neutrons from a nuclear weapon. Actually, since the spectrum of neutrons leaving a weapon is a strong function of its design, this assumption has the limitation that it represents the prompt neutron spectrum inside the bomb. However, this model is sufficiently accurate for the purposes of this discussion. The fast fission spectrum of U-235, as compared to the leakage spectrum of Godiva I, is shown in Figure 2.

Since it has been established that the dose rate and total dose received by an object exposed to a nuclear explosion is directly dependent upon the distance from such a burst, the reactor leakage spectrum must also be variable and easily degraded to lower energies to simulate this effect. In addition, it would be desirable to be

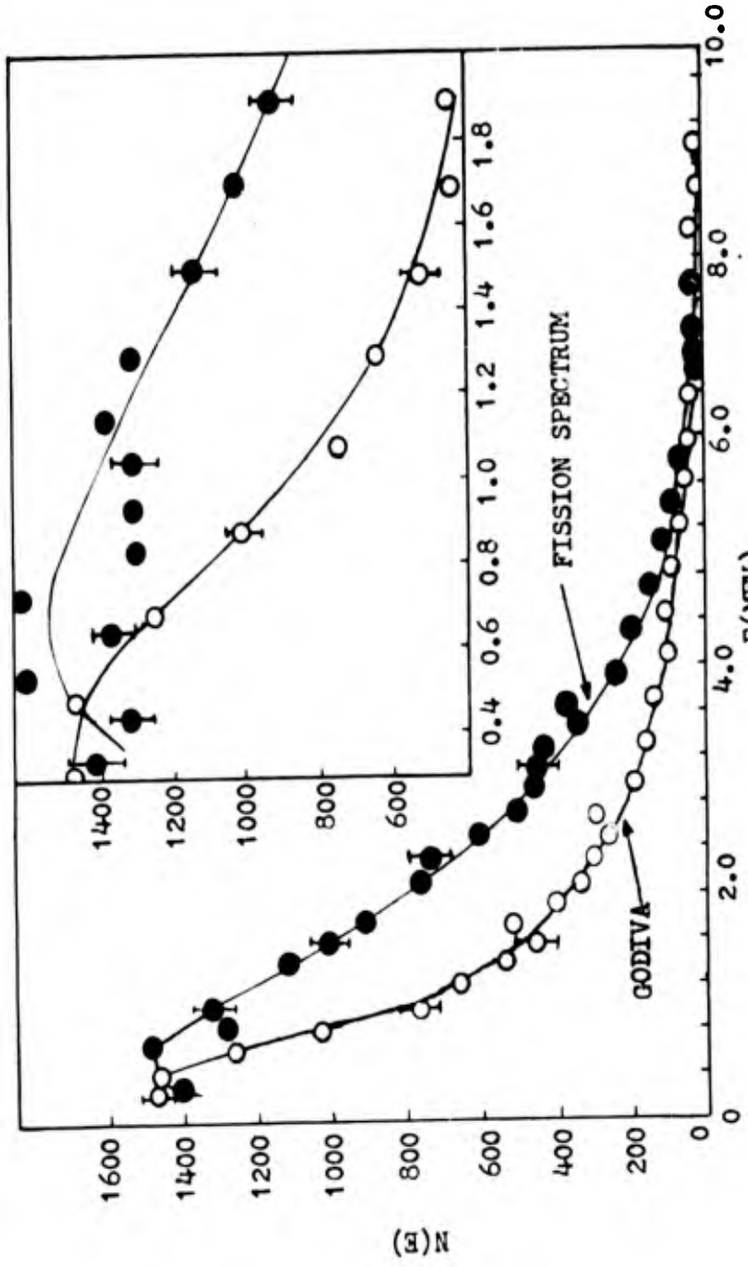

Fig. 2

Spectrum Comparison - Godiva I Leakage Spectrum and U_{235} Fission Spectrum (Ref. 34)

able to separate the neutron radiation from the gamma radiation or even to have a variable ratio of the two. However, these features do not have to be an integral part of the pulse reactor. Goals such as these can be easily achieved by the simple expedient of placing a calibrated absorption shield between the reactor and the object to be irradiated. The specific type or amount of absorption in the shield would be solely dependent upon the particular radiation desired. This would provide versatility in the system and permit a much broader scope in the demands of any specific experimental requirement.

Pulse Width

In order to simulate neutron and gamma-ray pulses at a short distance from a nuclear explosion, neutron doses must be very high and of short duration. Consequently, a pulse width that can be varied from 10 microseconds to several milliseconds is generally desired. The neutrons, from a nuclear burst, have a spread in velocity which introduces a time-of-flight broadening of the neutron pulse arriving at an object exposed to the burst. Since it is the pulse width at the object which must be matched or closely simulated, the requirement that the neutron doses be very high and of short duration is thus understandable. This time-of-flight broadening effect does not apply to gamma radiation since this radiation travels at the speed of light regardless of energy.

Total Neutron Yield

During the neutron pulse irradiation investigations conducted at the Godiva facilities, it was generally established that a total neutron yield of approximately 10^{17} neutrons per pulse, or larger, was required to attain the desired effects (Ref. 34). It was established that a flux of this magnitude would produce radiation effects similar to those caused by exposure to a nuclear burst. Consequently, a total neutron yield of approximately 10^{17} neutrons per pulse will be assigned as a design requirement of the proposed facility under consideration.

Time Interval Between Pulses

As a result of the increasing demand for the use of a pulsed reactor as an experimental tool in neutron pulse irradiation investigations and the expense of construction of these facilities, the time interval between pulses should be as short as possible compatible with the safe operation of the system. In the past, a large backlog of requests for experimental space around the Godiva reactors were piled up primarily because the time interval between pulses was so long. This time interval in the Godiva reactors was caused by the limitation placed on the systems by the maximum allowable temperature rise of 100° C. After a pulse was once initiated and consummated in the Godiva reactors, it was necessary that the reactor be allowed to cool prior to the initiation of a

subsequent pulse.

A pulse reactor designed to operate in a range of much higher temperatures with provisions for special cooling would permit shorter cooling periods and thus more pulsing operations in a given time interval. Consequently, the number of experimental investigations that can be conducted would be substantially increased. Therefore, as a result of this requirement, the configuration and composition of the reactor core must be selected on the basis of its stability and structural integrity at high temperature variations in addition to its nuclear properties.

Shut-down Mechanism

Since a high level of confidence is necessary in the safety of operation of a pulsing system, a pulse reactor must be designed with a large, prompt, negative reactivity temperature coefficient, i.e., built-in inherent shut-down mechanism. This would preclude or greatly decrease the possibility of an accidental generation of an uncontrollable neutron burst in case of malfunction. This built-in shut-down mechanism would not only assist in maintaining safe power levels, it would also reduce the number of control rods necessary to properly control the system. Therefore, with the number of rods decreased, the possibility of a malfunction occurring in the operation of such rods is virtually eliminated. Everything considered, such a negative temperature coefficient is

almost mandatory to assure the existence of proper safeguards throughout all phases of operation of a pulse facility.

Summary of Design Requirements

The general requirements for a pulse facility, based on the simulation of the radiation from a nuclear weapons burst, are as follows:

1. Neutron leakage spectra should be variable in its magnitude and energy ranges and should also be separable into neutron, gamma, or a variable ratio of these radiations.

2. Pulse widths should have a range of from 10 microseconds to several milliseconds.

3. The total neutron yield should be approximately 10^{17} neutrons per pulse.

Safety of operation, flexibility, and increased efficiency are the factors considered in the establishment of the requirements as listed below.

1. The reactor core should have a high heat capacity, good thermal conductivity, low thermal expansion, and, in addition, a high fuel concentration.

2. Time intervals between the ending of one pulse and the initiation of a subsequent pulse, should be as short as possible.

3. The pulse facility should have a large, prompt, negative reactivity temperature coefficient (built-in shut-down mechanism).

III. Design Proposals

In this section, the considerations involved in the selection of the configuration and composition of the proposed facility are discussed. The composition of highly-enriched U-10 w/o Mo is justified on the basis of its good mechanical and metallurgical characteristics at high temperatures in addition to its nuclear properties. Selection of the configuration was primarily based on a geometry that would minimize the induced stresses and resultant mechanical shocks which occur during a pulsing operation, in addition to the retention of a built-in shut-down mechanism similar to that of the Godiva reactors.

Composition

A fuel element composition that features a high fuel concentration, high heat capacity, good thermal conductivity, and a low thermal expansion is highly desired for utilization in a pulse reactor. Since high radiation flux and frequent elevated temperature cycling are also factors to be considered in the operation of this system, high temperature strength, phase stability, and dimensional stability are additionally desirable. Thus, for pulse reactor application, some metallic form of uranium, because of its mechanical and metallurgical properties, appears to be the most promising fuel.

Uranium. Pure uranium has three allotropic forms which have different lattice structures and different ranges of stability (Ref. 30). One form is orthorhombic in structure and designated alpha-uranium. In this phase, uranium is normally stable between room temperature and 668° C. Another form is referred to as beta-uranium. It has a tetragonal structure and it is generally stable between 668° C and 774° C. The third and last form is the gamma-uranium, a body-centered cubic in structure, which is stable from 774° C to the melting point (Fig. 3).

When exposed to thermal cycling, irradiation, or both, uranium metal undergoes changes such as surface roughening, anisotropic growth and the creation of internal voids. Most of this instability is due to the anisotropic structure of alpha-uranium, the phase normally present at room temperature. Efforts to reduce these effects are centered around stabilizing a phase which is relatively resistent to these same effects. This phase is gamma-uranium, which is normally unstable in pure uranium below 774° C. Fortunately, certain elements, when alloyed with alpha-uranium and properly heat treated, stabilize the gamma phase of uranium from room temperature up to the alloy melting point (Ref. 30). Since a number of elements will stabilize the gamma phase of uranium, the one imparting the best combination of stability, strength, fabricability, and nuclear properties for this particular application

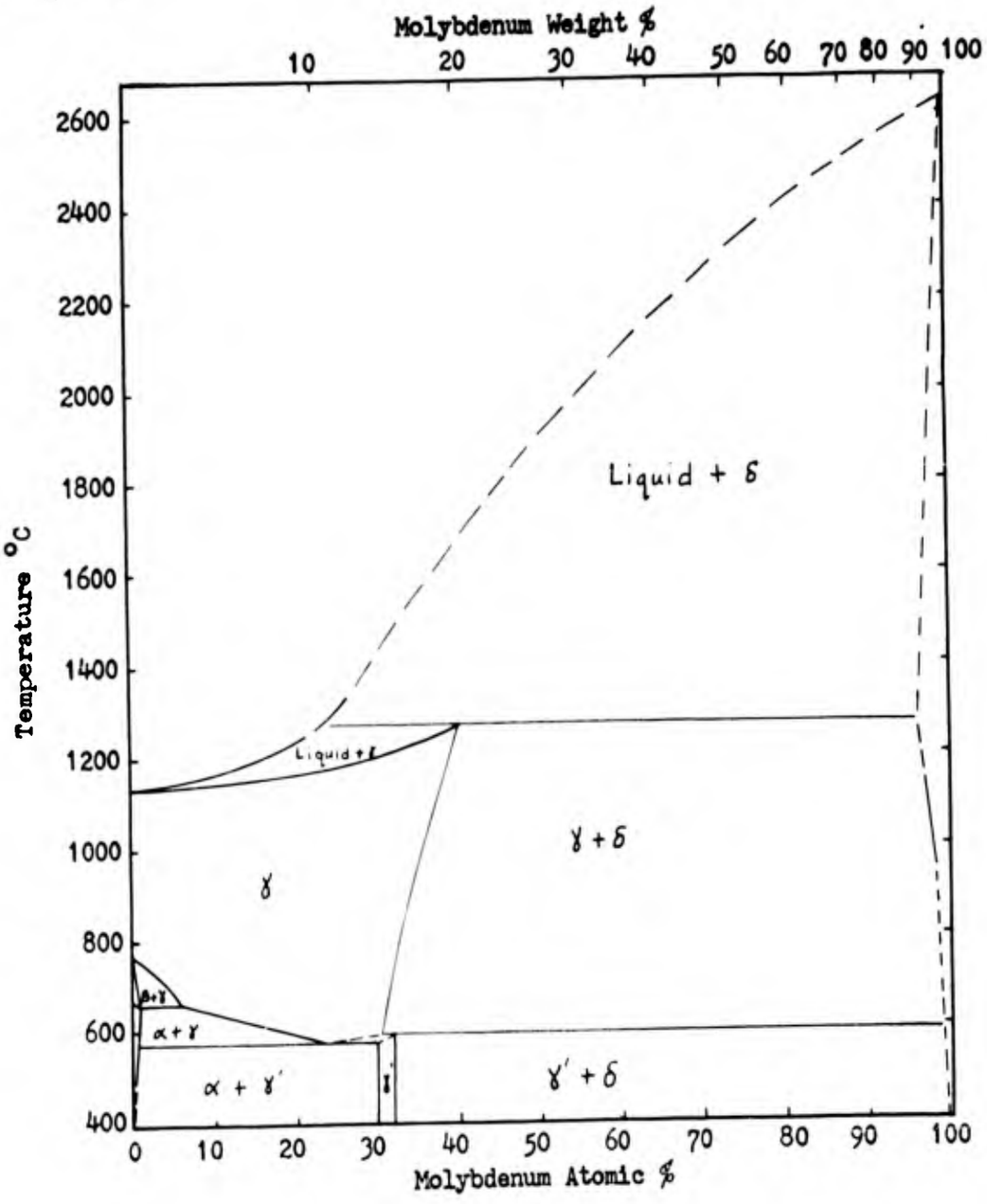

Figure 3

Uranium-molybdenum Phase Diagram (Ref. 30)

should be selected.

Uranium and 10% w/o Molybdenum. The most thoroughly investigated gamma-stabilized system is that of U-Mo up to about 15 w/o molybdenum. These investigations show that molybdenum in amounts around 10 w/o is an effective gamma-uranium stabilizing agent (Ref. 3). In addition to its gamma-phase stabilizing properties, the U-10 w/o Mo alloys have desirable mechanical and physical properties at room and elevated temperatures, and good thermal and radiation stability. Damage done by thermal cycling is greatly reduced by adding as low as 4.0 w/o Mo to uranium. Thus, the alloying of pure uranium with relatively small amounts of molybdenum greatly increases the usefulness of this fuel material beyond its former limits.

Fabrication procedures for the U-10 w/o Mo alloy are also well established. This alloy may be formed by most of the common fabrication methods such as rolling, casting, forging, and extrusion. Therefore, U-10 w/o Mo is a near-optimum material with respect to stability at desired fuel enrichments, mechanical performance, and ease of fabrication. Since by the most refined methods the enrichment of U-235 can only be accomplished up to 93.8%, the exact composition will be U-10 w/o Mo with an enrichment of 93.8% of U-235. Some of the properties of this alloy is listed in Table I.

Table I

Properties of U-10 w/o Mo Alloy*

Specific Heat	R.T.**	7.0 cal/mole/° C
	470° C	8.5 cal/mole/° C
	700° C	9.0 cal/mole/° C
Thermal Conductivity	R.T.	0.029 cal/cm-sec-° C
	800° C	0.091 cal/cm-sec-° C
Thermal Expansion	30° - 100° C	13.0×10^{-6} in/in/° C
	700°- 800° C	20.5×10^{-6} in/in/° C
Ultimate Strength	R.T.	142 - 140 ksi
	600° C	63 - 37 ksi
	800° C	8 - ksi
Yield Strength	R.T.	133 - 140 ksi
	600° C	54 - 30 ksi
Young's Modulus	R.T.	12.9×10^6 psi - 13.1
	600° C	9.5×10^6 psi - 4.3
	800° C	6.0×10^6 psi
Shear Modulus	0°	5.0×10^6 psi
	800°	2.0×10^6 psi

* Reference 7

** Room Temperature

Configuration

As mentioned previously, the primary difficulties encountered when pulsing a reactor are the stresses induced in the fuel elements. These stresses arise from the fact that the energy input is so rapid that the fuel elements cannot expand quickly enough to relieve them. In previous investigations, it has been determined that if the fuel elements were small and free to expand without interacting with each other, these stresses would be greatly reduced (Ref. 26). Consequently, the first consideration in the design of a pulse facility would be the selection of a geometrical configuration that would reduce the stress problem.

There are several methods that might be used to reduce the stress in the fuel elements, but the design that, first logic gives, appears also to be the most practical in terms of ease of fabrication, assembly, cooling, etc., is a core consisting of concentric cylindrical shells (see Fig. 1). If the spacing between the shells is small enough to have little effect on the neutronics of a cylindrical reactor and large enough to prevent interaction between the shells when undergoing thermal expansion, the induced stresses and inertial shock would be substantially decreased. This premise also presupposes that the shells themselves can be made thin enough to provide short, heat-transfer paths in order to limit the temperature gradients within the fuel elements.

Temperature Coefficient

Another important factor in the design problem would be the investigations relative to the existence of a large, prompt, negative temperature coefficient. When a sudden addition of excess reactivity is inserted in a just-critical reactor possessing an inherent limiting mechanism in the form of a negative reactivity temperature (or density) coefficient, the neutron level in the reactor, and hence its rate of generation of thermal energy, rises. As a result, the temperature in the reactor rises and the density decreases. This causes the neutron level and the power generation rate to decrease again to the level dictated by the steady state power capacity of the reactor.

In any reactor consisting of a multiplicity of fuel elements, extensive analytical and test work, involving the use of computers, would be necessary to establish the magnitude, or possibly the existence, of any substantial shut-down mechanism short of explosion. These complications arise from the fact that the rate at which the temperature coefficient becomes effective in shutting down the reactor is limited by the dynamics of expansion of the reactor and the coefficient with temperature itself. However, it is postulated that, as expansion occurs in the proposed layered structure, the shells expand in both directions until they are in very close proximity to each other and a shut-down mechanism similar

to, or better than, that of Godiva II is initiated. This would have to be proved by actual experimental tests prior to the time of critical assembly.

Summary of Design Proposals

To minimize the mechanical stresses in the core and still retain a built-in, shut-down mechanism, a layered structure of concentric, cylindrical shells has been proposed as a compromise design. In order to take full advantage of this configuration, the fuel elements should be composed of uranium and 10% w/o molybdenum. This alloy features good mechanical and metallurgical properties throughout the temperature range expected in the core during the operation of the pulse facility.

IV. Establishment of Bare Cylindrical Core Size

Obviously, the most useful information about a critical system is an accurate description of composition, shape, and size. Since the composition and configuration of the pulse facility has been established, this section will be concerned with the size and critical mass of a solid, bare, cylindrical reactor and will serve as the basis for the design configuration.

Most analytical methods used to determine the mass of a critical assembly give only approximations for this value. The only really accurate method for the determination of the critical mass is to perform a critical experiment. However, there are analytical methods that do give very close approximations to the exact amount of fuel material involved in a critical facility. For example, there are many computer codes established specifically for this analysis. Unfortunately, no readily available computers existed for this study, so the best available hand-calculation procedures had to be followed to obtain the first design estimates. In order to determine exactly what these procedures were, several methods were employed and tested against critical mass and dimensions of existing facilities, especially the Godiva I reactor. The method that gave the most accurate results involved the solution

to the Multigroup Asymptotic Transport Equation (Ref. 21). The results of this verification are covered in Appendix C.

Multigroup Asymptotic Transport Solution

In any volume element of a reactor, the rate of change of the neutron density with time is equal to the rate of production minus the rate of absorption and the rate of leakage (Ref. 13). The general equation representing the neutron balance is, therefore

$$\text{Production} - \text{Absorption} - \text{Leakage} = \frac{\partial n}{\partial t}, \tag{1}$$

where n is the neutron density and $\partial n/\partial t$ is its rate of change with time. When the system is at equilibrium, i.e., in a steady state, $\partial n/\partial t$ is zero; hence the steady-state equation is

$$\text{Absorption} + \text{Leakage} = \text{Production}. \tag{2}$$

If the reactor contains no extraneous neutron source, i.e., if the production of neutrons is due entirely to fission, then the steady state is equivalent to the critical state, and equation (2) is the critical equation. Consequently, the problem of obtaining the conditions for reactor criticality reduces itself to that of deriving expressions for the respective rates of production, absorption, leakage.

Production. In any reactor, the number of neutrons introduced into the system is proportional to the number of fissions, which, in

turn, is proportional to the flux of neutrons which produce fission. For any uniform reactor then, the source of neutrons will be proportional to the flux at each point. In the multigroup representation, the energy range of the fission neutrons is divided into an N number of smaller energy interval j, and all the neutrons are sorted into the same number of groups according to the energy interval into which they fall at the instant considered. A neutron of a given group is considered to exist at constant energy until a collision occurs, or until it leaks from the system. When a collision does occur, a neutron is either absorbed or it is scattered, either elastically or inelastically, into some lower energy group. Thus the source of neutrons in any given group is the sum of the fission neutrons born in this group and the number of neutrons scattered into this group from higher groups.

If those neutrons whose energy lies between two arbitrary limits E_j and E_{j-1} ($E_{j-1} > E_j$) are considered to make up the flux in group j, then the source term $S_j(r)$ may be written in the form

$$S_j(r) = \chi_j \sum_{R=1}^{N} \nu_k \Sigma_{f,R} \phi_R(r) + \sum_{l=1}^{j-1} \Sigma_{in}(l-j)\phi_l(r) + \sum_{m=1}^{j-1} \Sigma_{el\text{-}mod}(m-j)\phi_m(r) \quad (3)$$

where $S_j(r)$ = all neutrons born into group j at position r

χ_j = fraction of all fission neutrons born into group j

ν_k = total number of fission neutrons born per fission an any group k

$\sum_{f,k}$ = macroscopic fission cross section for group j

$\phi_k(r)$ = neutron flux in group k at position r

$\phi_\ell(r)$ = neutron flux in group ℓ at position r

$\phi_m(r)$ = neutron flux in group m at position r

$\sum_{in}(\ell \rightarrow j)$ = macroscopic cross section for scattering inelastically out of group ℓ into group j

$\sum_{el,mod}(m \rightarrow j)$ = macroscopic cross section for elastic moderation out of group m into group j.

This represents a source of neutrons which could be the result of fission by neutrons of any and all energies or the result of an energy-degradation process from some higher energy into the band between E_j and E_{j-1}.

The elastic moderation source, in principle, could have contributions from all higher energy groups; hence it has been summed from the highest energy group 1 to that just above group j. However, for materials other than hydrogen, such contributions are possible only from relatively nearby energy bands and frequently only from the next higher energy group (Ref. 9).

Absorption. Actually, in a multigroup calculation, total absorption in the entire system is just the sum of all the losses in each energy group. For example, a neutron that escapes absorp-

tion in one group is either degraded in energy and absorbed in a lower group or escapes the system entirely. Thus, it is convenient to define a total removal term that represents the total losses out of any specific group j. This term would represent the sum of all neutron loss mechanisms existing in a given energy interval.

In general, there are four mechanisms by which a neutron can be removed from an energy group. The four mechanisms of loss are complete capture, capture with resultant fissioning, inelastic scattering into a lower group, and elastic moderation into a lower group. Of course, in addition to these, a neutron could be lost through leakage, but this will be considered in the next section.

If the same assumption is made that the flux in group j is made up of the neutrons whose energy lies between E_j and E_{j-1}, the total losses as a result of these mechanisms can be represented by

$$\sum_{removal} \phi_j(r) = (\Sigma_{c,j} + \Sigma_{f,j} + \Sigma_{in,j} + \Sigma_{el\text{-}mod,j})\phi_j(r) \quad (4)$$

where $\phi_j(r)$ has the same meaning as before and

$\Sigma_{c,j}$ = macroscopic capture cross section for group j

$\Sigma_{f,j}$ = macroscopic fission cross section for group j

$\Sigma_{in,j}$ = macroscopic cross section for scattering inelastically out of group j

$\Sigma_{el\text{-}mod,j}$ = macroscopic cross section for elastic moderation out of group j

Thus,

$\Sigma_{removal,j} = \Sigma_{c,j} + \Sigma_{f,j} + \Sigma_{in,j} + \Sigma_{el\text{-}mod,j}$ = the total macroscopic cross section for processes removing neutrons from group j.

Leakage. The determination of leakage is not quite as simple as the other mechanisms of loss. Leakage arises from the fact that neutrons are in motion; consequently more neutrons will, on the average, leave the reactor, where the neutron density or concentration is high, than will return to it from the surrounding space, where the density is low. In actual practice the neutron motion is affected by collisions with atomic nuclei which cause scattering to occur; this plays a major role in neutron diffusion upon which the calculation of leakage is based.

If multigroup diffusion theory is applied to a bare reactor core, the neutron leakage can be represented by

$$D_j \nabla^2 \phi(r) \tag{5}$$

where D_j is defined as the diffusion coefficient (Ref. 13). Furthermore, if one simplifying assumption is made, the spatial dependence of the above expression is removed and an analytical solution is made possible which is particularly adaptable for hand

calculations. The basic hypothesis is that the flux has the same shape in every group. This is not rigorously true, since this implies that the extrapolation distance is the same for all energy groups. However, in a bare core, this assumption of a space-independent neutron energy spectrum gives results which are fairly accurate away from the boundaries of the system (Ref. 9). Thus, it is assumed that

$$\phi_j(r) = \phi_j F(r) \tag{6}$$

where F(r) is a spatial shape factor independent of the energy. If it is further assumed that

$$\nabla^2\phi(r) = -B^2\phi(r) \tag{7}$$

where B^2 is the material buckling, and

$$\nabla^2 F(r) = -B^2 F(r) \tag{8}$$

then the total leakage from group j would be simply

$$-D_j B^2 \phi_j \tag{9}$$

and the spatial dependence has been completely removed.

Summation. With the assumptions as made in the previous sections, the neutron balance equation in a steady state condition becomes

$$\text{Production} = \text{Losses} \tag{10}$$

or

$$-D_j B^2 \phi_j - \Sigma_{\text{removal},j}\phi_j + \chi_j \sum_{k=1}^{N} \nu_k \Sigma_{f,k}\phi_k + \sum_{l=1}^{j-1} \Sigma_{in}(l\to j)\phi_l + \sum_{m=1}^{j-1} \Sigma_{el\text{-}mod}(m\to j)\phi_m = 0 \tag{11}$$

If (11) is rearranged, the value for the flux in group j is represented by

$$\phi_j = \frac{\chi_j \sum_{k=1}^{N} \nu_k \Sigma_{f,k}\phi_k + \sum_{l=1}^{j-1} \Sigma_{in}(l\to j)\phi_l + \sum_{m=1}^{j-1} \Sigma_{el\text{-}mod}(m\to j)\phi_m}{D_j B^2 + \Sigma_{\text{removal},j}} \tag{12}$$

Although the flux in group j as represented by (6) and (12) is fairly representative of the flux distribution in thermal or large reactors, it does not represent too well the flux distribution in a small fast reactor like a Godiva. Consequently, it is necessary to modify this concept in order to obtain values that are more in line with the flux distribution as it really exists in a fast assembly. Since this modification involves only the leakage term, the loss mechanisms are the only ones of concern and the source terms all remain the same. According to transport theory (Ref. 21), if the physical dimensions of a fast reactor is of the same order

of magnitude as the transport mean free path of the neutrons causing fissions, then the total losses from any group j is given by

$$\frac{B\phi_j}{\frac{\tan^{-1}B}{\Sigma_{tr,j}}} - \Sigma_{el\text{-}tr,j}\phi_j \qquad (13)$$

where

B = square root of the material buckling

$\Sigma_{tr,j}$ = macroscopic transport cross section in j group

$\Sigma_{el\text{-}tr,j} = \Sigma_{tr,j} - \Sigma_{removal,\,j} = \Sigma_{tr,j} - \Sigma_{c,j} - \Sigma_{f,j} - \Sigma_{in,j} - \Sigma_{el\text{-}mod,j}$ = elastic macroscopic transport cross section in group j.

With this modification to the loss of neutrons out of any group j, then ϕ_j is now determined by

$$\phi_j = \frac{\chi_j \sum_{k=1}^{N} \nu_k \Sigma_{f,k}\phi_k + \sum_{l=1}^{j-1} \Sigma_{in}(l\to j)\phi_l + \sum_{m=1}^{j-1} \Sigma_{er}(m\to j)\phi_m}{\frac{B}{\frac{\tan^{-1}B}{\Sigma_{tr,j}}} - \Sigma_{el\text{-}tr,j}} \qquad (14)$$

which is the Multigroup Asymptotic Transport Equation. In this equation, the elastic transport cross section $\Sigma_{el\text{-}tr,j}$, which

appears in the denominator, implies that a fraction of the total neutrons elastically scattered in group j does not leave the group, therefore, these neutrons do not contribute to the leakage.

Cross Section.* The first step in the solution of Equation (14) is to determine how many energy groups should be used and if the cross sections for these energy intervals are available. A survey of the literature reveals that there is a preponderance of these cross sections for some materials and a definite lack for others. Uranium, for example, has cross sections listed by innumerable authors and for many different energy groups, while molybdenum cross sections are very difficult to come by. In addition, these cross sections are usually compiled from empirical data collected from experimental evidence and the values thus listed, for the same number of energy groups, vary from author to author.

Since these cross sections represent an average value for the energy interval considered, it logically follows that the accuracy of these values increase as the number of groups increase. However, a six-group calculation is usually sufficient to give results within the limits of error of a hand calculation. Nevertheless,

---

* In these paragraphs, the term "cross section" signifies "microscopic cross section."

it is still necessary to check the validity of the cross sections used against the known parameters of an existing facility.

In this particular investigation, the six-group cross sections given by ANL-5800 (Ref. 25) for U-235 and U-238, were used to solve for the critical mass of Godiva and excellent results were obtained. Unfortunately, there were no cross sections listed for molybdenum in the six-energy-group interval. These cross sections were eventually obtained from a Mr. Kinney at Oak Ridge National Laboratories. When these cross sections were received, they had a note attached to the effect that the cross sections conformed in notation to those as listed for uranium in LAMS 2255. Therefore, these cross sections were extracted from this report and another iteration was completed, using Godiva as a model. However, the results obtained were so far in error that the cross sections as listed by LAMS 2255 had to be discarded.

At this point, an attempt was made to match the cross sections for molybdenum received from Mr. Kinney to those as given by ANL-5800 and another interation was performed in an effort to establish the critical mass of a bare cylindrical core composed of U-10 w/o Mo. However, these results were also far above what logic indicated that it should be. Consequently, the six-group cross sections had to be discarded altogether.

Fortunately, the cross sections for U-235, U-238, and Mo,

for eleven energy groups, are all tabulated in ANL-5800. When these cross sections were checked, again using Godiva as a model, the results obtained were very good. Therefore, these cross sections were used for all subsequent iterations. The cross sections for U-235, U-238, and Mo are all shown in Tables II, III, and IV respectively. The notation in these tables conforms to that of ANL-5800 (Ref. 25) and the definitions are contained in Appendix A.

Procedure for Solution. Before the iteration process can be started, it is necessary to convert the microscopic cross sections, discussed in the last section, to the macroscopic cross sections used in the solution of Equation (14). The group macroscopic cross sections may be obtained from the corresponding microscopic group cross sections for individual materials, i.e., for reaction q in material z (Ref. 25),

$$\sum_{q,j} = \sum_{z} N^{z} \sigma_{q,j}^{z} \tag{15}$$

where N^z = atoms/cm^3 of material z

$\sigma_{q,j}^{z}$ = microscopic cross section for reaction q in group j for material z

Table V contains the values for the appropriate group macroscopic cross sections involved in this analysis.

Table II

Uranium - 235
Microscopic Cross Sections in Barns*
(11 Energy Groups)

j	E_L(Mev)	χ_j	σ_{tr}	ν	j
1	2.25	0.338	4.5	2.77	1
2	1.35	0.236	4.5	2.65	2
3	0.825	0.178	4.8	2.58	3
4	0.5	0.116	5.1	2.53	4
5	0.3	0.066	6.3	2.51	5
6	0.18	0.033	7.9	2.49	6
7	0.11	0.017	9.65	2.48	7
8	0.067	0.008	10.9	2.47	8
9	0.025	0.006	12.25	2.47	9
10	0.0091	0.002	13.5	2.47	10
11	0	0	14.3	2.47	11

* Reference 25

Table II (Continued)

j	σ_f	σ_c	σ_{er}	σ_{in}	j
1	1.3	0.1001	0.00941	2.3	1
2	1.28	0.0998	0.0192	1.85	2
3	1.25	0.10	0.0386	1.15	3
4	1.20	0.144	0.0429	1.2	4
5	1.28	0.192	0.0694	0.7	5
6	1.42	0.2256	0.0978	0.4	6
7	1.6	0.32	0.130	0	7
8	1.9	0.475	0.143	0	8
9	2.3	0.69	0.0778	0	9
10	3.4	1.19	0.0748	0	10
11	6.0	2.52	0	0	11

Table II (Continued)

j	$\sigma_{in}(j \rightarrow j+k)$						j
	k = 1	2	3	4	5	6	
1	0.881	0.660	0.382	0.207	0.115	0.0552	1
2	0.845	0.488	0.265	0.144	0.0712	0.0361	2
3	0.544	0.294	0.161	0.0805	0.0402	0.0299	3
4	0.576	0.314	0.157	0.0798	0.0582	0.0144	4
5	0.351	0.175	0.0896	0.0649	0.0155	0.00434	5
6	0.200	0.103	0.0744	0.0176	0.0048	0	6
7	0	0	0	0	0	0	7
8	0	0	0	0	0	0	8
9	0	0	0	0	0	0	9
10	0	0	0	0	0	0	10
11	0	0	0	0	0	0	11

Table III

Uranium - 238
Microscopic Cross Sections in Barns*
(11 Energy Groups)

j	σ_{tr}	ν	σ_f	σ_c	σ_{er}	σ_{in}	j
1	4.7	2.65	0.59	0.015	0.0144	2.87	1
2	4.5	2.55	0.45	0.062	0.0234	2.44	2
3	5.0	2.47	0.003	0.13	0.0616	1.20	3
4	5.5	0	0	0.143	0.0826	0.44	4
5	6.7	0	0	0.13	0.102	0.47	5
6	8.25	0	0	0.15	0.127	0.55	6
7	9.65	0	0	0.20	0.150	0.55	7
8	10.9	0	0	0.30	0.171	0.40	8
9	12.25	0	0	0.40	0.0991	0.05	9
10	13.5	0	0	0.61	0.108	0	10
11	14.3	0	0	0.80	0	0	11

* Reference 25

Table III (Continued)

j	$\sigma_{in}(i \to i+k)$						j
	k = 1	2	3	4	5	6	
1	1.06	0.46	0.66	0.39	0.12	0.18	1
2	0.62	0.89	0.52	0.16	0.10	0.15	2
3	0.52	0.35	0.22	0.11	0	0	3
4	0.44	0	0	0	0	0	4
5	0.47	0	0	0	0	0	5
6	0.50	0.05	0	0	0	0	6
7	0.55	0	0	0	0	0	7
8	0.38	0.02	0	0	0	0	8
9	0.03	0.02	0	0	0	0	9
10	0	0	0	0	0	0	10
11	0	0	0	0	0	0	11

Table IV

Molybdenum
Microscopic Cross Sections in Barns*
(11 Energy Groups)

j	σ_{tr}	σ_t	σ_{in}	$\sigma_{in}(i \to i+k)$						j
				k=1	2	3	4	5	6	
1	2.5	0.010	1.40	0.35	0.40	0.30	0.15	0.10	0.10	1
2	3.2	0.017	0.84	0.411	0.33	0.099	0	0	0	2
3	4.0	0.024	0.40	0	0.108	0.117	0.068	0.042	0.065	3
4	5.3	0.034	0	0	0	0	0	0	0	4
5	6.4	0.040	0	0	0	0	0	0	0	5
6	7.2	0.046	0	0	0	0	0	0	0	6
7	7.8	0.057	0	0	0	0	0	0	0	7
8	7.9	0.066	0	0	0	0	0	0	0	8
9	7.4	0.090	0	0	0	0	0	0	0	9
10	7.1	0.120	0	0	0	0	0	0	0	10
11	7.2	0.200	0	0	0	0	0	0	0	11

* Reference 25

Table V

Macroscopic Cross Sections in Barns
(11 Energy Groups)

N_1 (U-235) = 0.03744×10^{24} atoms/cm^3

N_2 (U-238) = 0.0025×10^{24} atoms/cm^3

N_3 (Mo) = 0.0102×10^{24} atoms/cm^3

j	$\Sigma_{tr,j}$	$\Sigma_{el-tr,j}$	$\Sigma_{er}(j \to j+1)$	j
1	0.20541	0.05083	0.00039	1
2	0.21205	0.07446	0.00098	2
3	0.23268	0.13000	0.00159	3
4	0.25840	0.15996	0.00181	4
5	0.31746	0.23154	0.00285	5
6	0.33398	0.30665	0.00397	6
7	0.46430	0.37964	0.00524	7
8	0.51516	0.41214	0.00598	8
9	0.56388	0.44695	0.00316	9
10	0.61067	0.43333	0.00307	10
11	0.64358	0.32115	-	11

Table V (Continued)

j	$\sum_{in}(1\to j)$	$\sum_{in}(2\to j)$	$\sum_{in}(3\to j)$	$\sum_{in}(4\to j)$	$\sum_{in}(5\to j)$	j
1	-	-	-	-	-	1
2	0.03914	-	-	-	-	2
3	0.02989	0.03732	-	-	-	3
4	0.01899	0.02384	0.02163	-	-	4
5	0.01025	0.01221	0.01297	0.02263	-	5
6	0.00562	0.00578	0.00776	0.01173	0.01430	6
7	0.00353	0.00291	0.00398	0.00587	0.00654	7
8	0	0.00173	0.00193	0.00298	0.00335	8
9	0	0	0.00178	0.00217	0.00243	9
10	0	0	0.00159	0.00054	0.00058	10
11	0	0	0	0	0.00016	11

Table V (Continued)

j	$\sum_{in}(6\to j)$	$\sum_{in}(7\to j)$	$\sum_{in}(8\to j)$	$\sum_{in}(9\to j)$	$\sum_{in}(10\to j)$	i
1	-	-	-	-	-	1
2	-	-	-	-	-	2
3	-	-	-	-	-	3
4	-	-	-	-	-	4
5	-	-	-	-	-	5
6	-	-	-	-	-	6
7	0.00872	-	-	-	-	7
8	0.00398	0.00138	-	-	-	8
9	0.00278	0	0.00095	-	-	9
10	0.00066	0	0.00005	0.00008	-	10
11	0.00018	0	0	0.00005	0	11

After the above values are obtained, Equation (14) can be considered as a set of N simultaneous equations, one for each group. Since there are no contributions to the highest energy group, i.e., j = 1, from inelastic or elastic moderation processes, the numerator of Eq (14) consists only of the fission source. If ν_k is assumed to be constant for all energy groups causing fissions, then it can also be assumed that the total fission source for all groups $\sum_{k=1}^{N} \nu_k \Sigma_{f,k} \phi_k$ is some arbitrary number, say unity, and ϕ_1 is given by

$$\phi_1 = \frac{\gamma_1}{\frac{B}{\tan^{-1}\frac{B}{\Sigma_{tr,1}}} - \Sigma_{el-tr,1}} \tag{16}$$

The procedure for solution is an iterative process, where B is the quantity which will be iterated on. The first step in the solution is to guess some reasonable value for B, by say a one group approximation, and then solve for ϕ_1, from Eq (16). After ϕ_1, has been determined with the trial value of B, then it is possible to evaluate ϕ_2:

$$\phi_2 = \frac{\gamma_2 + \Sigma_{in(1\to 2)}\phi_1 + \Sigma_{el-mod(1\to 2)}\phi_1}{\frac{B}{\tan^{-1}\frac{B}{\Sigma_{tr,2}}} - \Sigma_{el-tr,2}} \tag{17}$$

Since this group gets source neutrons, other than fission, only from group 1, ϕ_2 is completely specified and can be calculated. This process is continued through all the groups in numerical order in this fashion. After N values of ϕ_j has been obtained, a convergence test is applied. A value for the total fission source $\sum_{k=1}^{N} \nu_k \Sigma_{f,k} \phi_k$ is calculated and compared to the original assignment of unity. The equations are solved if the two agree within the desired limits of accuracy. Otherwise, a new guess on B is made and a second iteration performed. After the second set of ϕ_j's have been calculated, the fission source is again computed and compared with unity. This process is repeated until the two converge. When the solution does converge, the critical value of the material buckling may be determined by squaring the value of B thus obtained. If a bare core of this material was built in any geometrically calculable shape, its extrapolated dimensions would have to be such that the geometric buckling equaled this material buckling at criticality.

When the solution is complete, not only the material buckling B^2, but also the neutron energy spectrum has been determined. The spectrum is, of course, given by the relative values of the total flux ϕ_j in each energy band.

Numerical Results

Following the iterative method of solution for the Multigroup

Asymptotic Transport Equation for eleven groups, the final value for B was determined to be 0.280 and consequently, $B^2 = 0.0784$ (see Sample Calculations Appendix B). The numerical values for ϕ_j and the other parameters involved were found to be as indicated in Table VI.

Extrapolated Dimensions. Since the material buckling has been determined, the geometric buckling of a solid bare cylinder must equal it, in clean-cold status, in order for the assembly to be in a critical configuration. The geometric buckling is given by

$$B^2 = \frac{\pi^2}{\tilde{H}^2} + \frac{(2.405)^2}{\tilde{R}^2} \qquad (18)$$

where $\tilde{R}$ = extrapolated radius of cylinder

$\tilde{H}$ = extrapolated height of cylinder.

To solve for $\tilde{R}$ or $\tilde{H}$ in (18), the ratio of height $\tilde{H}$ to radius $\tilde{R}$ must be arbitrarily specified. It has been shown that the ratio that gives the minimum volume of the cylinder is when $\tilde{H}/\tilde{D} \approx 1.1$ or $\tilde{H} \approx 2.2R$ (Ref. 12). Making these substitutions, $\tilde{R}$ was computed to be 10.02 cm and $\tilde{H}$ = 22.04 cm.

Physical Dimensions. The extrapolated distance of a fast reactor, i.e., the distance outside the boundary at which point the flux is assumed to go to zero, has been measured experimentally for heavy fuel concentrations, such as the system under consideration,

Table VI

Multigroup Asymtotic Transport Solution
(Final Iteration)

B = 0.280

j	S_j*	$\sum_{in}(1\to j)\phi_1$	$\sum_{in}(2\to j)\phi_2$	$\sum_{in}(3\to j)\phi_3$	j
1	0.338	-	-	-	1
2	0.236	0.053111	-	-	2
3	0.178	0.040559	0.046918	-	3
4	0.116	0.025768	0.029971	0.030266	4
5	0.066	0.013909	0.015350	0.018148	5
6	0.033	0.007626	0.007266	0.010358	6
7	0.017	0.004790	0.003658	0.005569	7
8	0.008	0	0.002175	0.002701	8
9	0.006	0	0	0.002491	9
10	0.002	0	0	0.002225	10
11	0	0	0	0	11

* $\sum S_j$ = 1.00000

Table VI (Continued)

j	$\sum_{in}(4\to j)\phi_4$	$\sum_{in}(5\to j)\phi_5$	$\sum_{in}(6\to j)\phi_6$	$\sum_{in}(7\to j)\phi_7$	j
1	-	-	-	-	1
2	-	-	-	-	2
3	-	-	-	-	3
4	-	-	-	-	4
5	0.025611	-	-	-	5
6	0.013275	0.012850	-	-	6
7	0.006643	0.005877	0.007960	-	7
8	0.003373	0.003010	0.003633	0.000554	8
9	0.002456	0.002184	0.002538	0	9
10	0.000611	0.000521	0.000603	0	10
11	0	0.000144	0.000164	0	11

Table VI (Continued)

j	$\sum_{in}(8\to j)\phi_8$	$\sum_{in}(9\to j)\phi_9$	$\sum_{in}(10\to j)\phi_{10}$	$\sum_{el\text{-}mod}(j\to j+1)$	j
1	-	-	-	0.000529	1
2	-	-	-	0.000981	2
3	-	-	-	0.002225	3
4	-	-	-	0.002048	4
5	-	-	-	0.002561	5
6	-	-	-	0.003624	6
7	-	-	-	0.002105	7
8	-	-	-	0.001011	8
9	0.000161	-	-	0.000330	9
10	0.000008	0.000008	-	0.000089	10
11	0	0.000005	0	-	11

Table VI (Continued)

j	$S_j + \sum_{\ell=1}^{j-1} \Sigma_{in}(\ell \to j)\phi_\ell$ *	$\Sigma_{el-tr,j}$	$\Sigma_{tr,j}$	$B/\Sigma_{tr,j}$	j
1	0.338000	0.05083	0.20541	1.37580	1
2	0.289640	0.07446	0.21205	1.33270	2
3	0.266458	0.13000	0.23268	1.21450	3
4	0.204230	0.15996	0.25840	1.09370	4
5	0.141066	0.23154	0.31746	0.89019	5
6	0.087436	0.30665	0.33398	0.84616	6
7	0.055121	0.37964	0.46430	0.60866	7
8	0.025510	0.41214	0.51516	0.54857	8
9	0.016841	0.44695	0.56388	0.50117	9
10	0.006306	0.43333	0.61067	0.46277	10
11	0.000402	0.32115	0.64358	0.43911	11

* $\Sigma_{in}(\ell \to j)$ includes $\Sigma_{el-mod}(\ell \to j)$

Table VI (Continued)

j	$\mathrm{Tan}^{-1} B/\Sigma_{cr,j}$	$B/\mathrm{Tan}^{-1}(B/\Sigma_{cr,j})$	$[B/\mathrm{Tan}^{-1}(B/\Sigma_{cr,j})]-\Sigma_{cl-cv,j}$	ϕ_j	j
1	0.94226	0.29992	0.24909	1.35694	1
2	0.92700	0.30485	0.23039	1.25717	2
3	0.88193	0.32043	0.19043	1.39924	3
4	0.83014	0.34042	0.18046	1.13172	4
5	0.72735	0.38853	0.15699	0.89857	5
6	0.70224	0.40243	0.09578	0.91288	6
7	0.54675	0.51687	0.13723	0.40167	7
8	0.50174	0.56324	0.15110	0.16910	8
9	0.46457	0.60830	0.16135	0.10438	9
10	0.43341	0.65204	0.21871	0.02883	10
11	0.41375	0.68302	0.36187	0.00111	11

$$\sum S_i = 1.00000$$

$$\sum_{R=1}^{N} \nu_R \Sigma_{f,R} \Phi_R = 0.99772$$

Converges

and tabulated (Ref. 25). Since there is no really good theoretical method for the determination of this value for fast reactors (Ref. 31), the tabulated value for this particular degree of enrichment was assumed to be representative of this system. The value thus obtained for the extrapolated distance was 2.08 cm. Consequently, the physical radius and height of the solid bare cylinder was computed to be $R = 7.94$ cm and $H = 17.88$ cm. The resultant volume was 3542.07 cc and the resultant critical mass was 55.22 kg.

Summary

The material buckling of a solid bare cylinder composed of U-10 w/o Mo was determined by using the multigroup asymptotic transport iteration procedure. The value thus obtained was equated to the geometric buckling of a cylinder and the physical dimensions were computed. From these dimensions, the resultant volume and critical mass was determined. The appropriate values for these parameters are as follows:

$$B^2 = 0.078$$

$$R = 7.94 \text{ cm}$$

$$H = 17.88 \text{ cm}$$

$$V_c = 3542.07 \text{ cc}$$

$$M_c \quad 55.22 \text{ kg}$$

V. Introduction of Voids

The primary objective of having concentric axial voids in the pulse reactor is to relieve or breakup the mechanical stresses and inertial shock during a pulsing cycle and secondarily to provide a means for expedient cooling of the system. Consequently, the size of the voids is chiefly dependent upon the maximum thermal expansion that occurs throughout the temperature ranges of operation. As a first approximation, it will be assumed that the system expands linearly in the radial and axial directions. Naturally, the maximum thermal expansion will occur near the center of the core and, if the size of the annular voids are based on this maximum value, the size of the voids near the boundaries will be more than adequate. Based on the melting point of the U-10 w/o Mo alloy, the pulse reactor will be limited to a rise of 800° C.

In addition to the annular voids, it will be necessary to provide some means for pulsing the system. The method that presents a simple means of pulsing is to provide the reactor with a central "glory hole" into which the excess reactivity may be introduced in the form of additional fuel (Fig. 4). In the subsequent sections, the effect of introducing these voids into the solid bare cylindrical core will be analyzed and the new critical dimensions and mass determined.

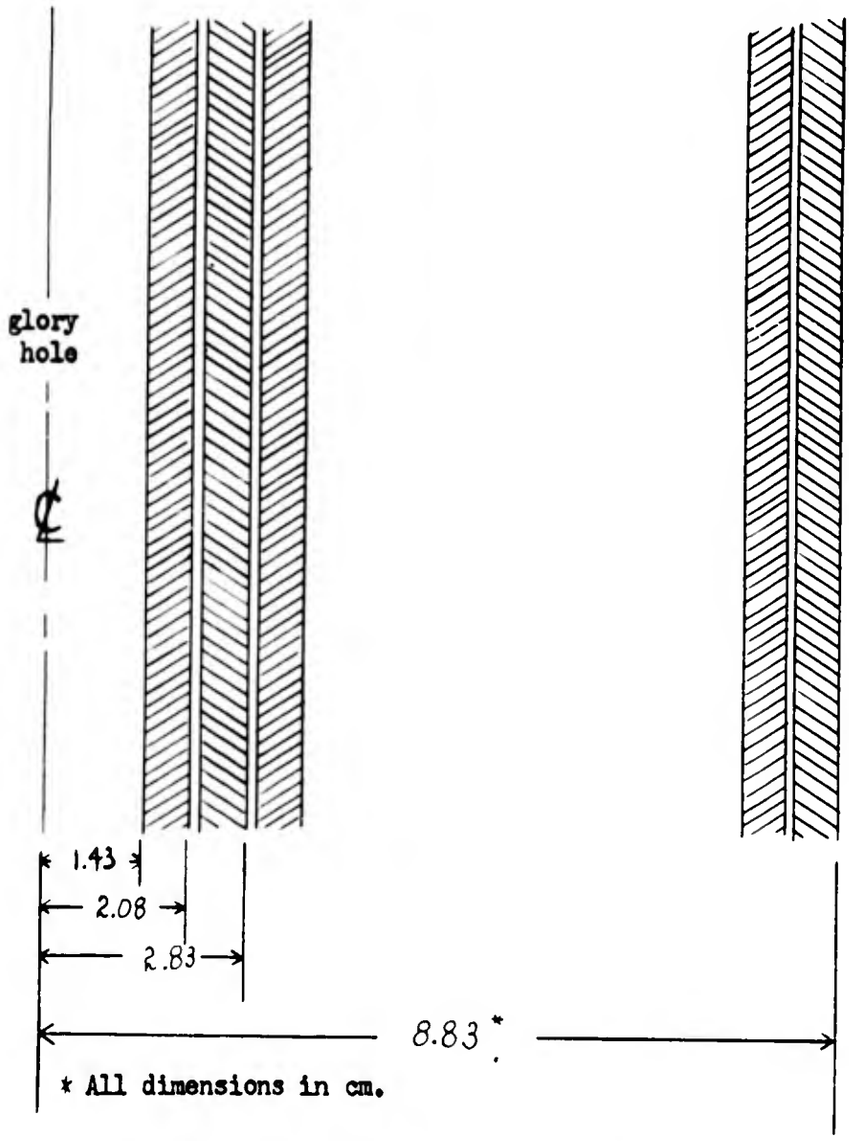

Figure 4

Configuration of Core

Size of Voids

Since it has been assumed that the thermal expansion is linear, the maximum radial expansion may be derived from the expression

$$\alpha = \frac{1}{R_o} \frac{R - R_o}{T - T_o} = \frac{\Delta R}{R_o \Delta T}$$

Where ΔR = change in radius as a result of ΔT

ΔT = temperature rise

α = thermal coefficient of expansion

R_o = radius prior to ΔT

Therefore, by using the known value for the thermal expansion coefficient, the maximum thermal expansion for a 800° C rise in temperature can be computed. The coefficient of expansion for U-10 w/o Mo was presented in Table I and has a value of 20.5×10^{-6} in/in/° C in the maximum temperature range. Thus, for a temperature rise of 800° C, the maximum expansion for one inch in the radial direction is 0.0164 in, or, to allow for expansion in both directions, this value can be doubled to give a value of 0.0328 in. Consequently, the spacing between the shells will be established as a value slightly larger than this to prevent contact. An arbitrary value of 0.04 in or 0.10 cm can now be assumed to be the radial spacing between the shells composing the core.

The size of the "glory hole" will be assigned on the basis of

the necessary size of the fuel rod to maintain its structural integrity throughout the cycling operation and the necessary clearance between the rod and the cylinder wall to prevent binding or malfunction. It has been established that a fuel rod of 1 in diameter will maintain the necessary integrity (Ref. 1). Therefore, the "glory hole" should be at least 1.125 in or 2.86 cm.

Effect of Voids on Critical Dimensions

The effect of the voids on the critical dimensions of a cylindrical reactor of finite height is determined by solving the wave equation, i.e.,

$$\nabla^2\phi(r,\theta,z) + B^2\phi(r,\theta,z) = 0 \qquad (19)$$

and introducing new boundary conditions to the solution.

In the treatment of a cylindrical reactor of finite height, if the z axis is made to coincide with the vertical axis of the cylinder, only the z and r coordinates need to be considered and the wave equation becomes

$$\frac{\partial^2\phi}{\partial r^2} + \frac{1}{r}\frac{\partial\phi}{\partial r} + \frac{\partial^2\phi}{\partial z} + B^2\phi = 0 \qquad (20)$$

The boundary conditions of the problem are that $\phi(r,z)$ shall be finite and that it shall go to zero at the extrapolated boundaries, i.e., when $r = \tilde{R}$ or $z = \tilde{H}/2$, the origin being taken at mid-

way up the cylinder of height H. In addition, it will be further assumed that no scattering or absorption takes place in the voids, thus $\phi(r,z)$ is constant inside the central channel and in the annular voids (see Fig. 6).

The solution of (20) is performed by first separating the variables r and z by writing

$$\phi(r,z) = \Theta(r)Z(z) \tag{21}$$

so that (20) becomes, after dividing by ΘZ,

$$\frac{1}{\Theta}\left(\frac{d^2\Theta}{dr^2} + \frac{1}{r}\frac{d\Theta}{dr}\right) + \frac{1}{Z}\frac{d^2Z}{dz^2} + B^2 = 0 \tag{22}$$

in which the first term depends on Θ only, and the second term on Z only; each of the terms can consequently be set equal to a constant. Let

$$\frac{1}{\Theta}\left(\frac{d^2\Theta}{dr^2} + \frac{1}{r}\frac{d\Theta}{dr}\right) = -\alpha^2 \tag{23}$$

where α^2 is a constant. Similarly, let

$$\frac{1}{Z}\frac{d^2Z}{dz^2} = -\beta^2 \tag{24}$$

where β^2 is also a constant. Consequently, by (22)

$$B^2 = \alpha^2 + \beta^2 \tag{25}$$

By rearranging (23), and multiplying through by Θr^2 , the result is

$$r^2 \frac{d^2\Theta}{dr^2} + r \frac{d\Theta}{dr} + \alpha^2 r^2 \Theta = 0 \tag{26}$$

The general solution of (26) is

$$\Theta = A J_0(\alpha r) - C Y_0(\alpha r) \tag{27}$$

where J_0 and Y_0 are Bessel functions of the first and second kinds, respectively, of zero order (Ref. 12).

In order to evaluate α , use is made of the boundary conditions that $\phi(r,z)$ shall go to zero at the extrapolated boundary, i.e., when $r = \tilde{R}$, and that the flux is constant in the voids. Since $\Theta(r)$ represents the part of $\phi(r,z)$ which is dependent on r, it follows from (27) that

$$\Theta(r) = A J_0(\alpha \tilde{R}) - C Y_0(\alpha \tilde{R}) = 0 \tag{28}$$

$$\left.\frac{d\Theta(r)}{dr}\right]_{r=R_0} = A J_0'(\alpha R_0) - C Y_0'(\alpha R_0) = 0 \tag{29}$$

where R_0 = radius of the central channel, and

$$\left.\frac{d\Theta(r)}{dr}\right]_{r=\Delta R} = A J_o'(\alpha \Delta R) - C Y_o'(\alpha \Delta R) = 0 \qquad (30)$$

where $\Delta R = r_1 - r_2 = r_3 - r_4$, etc., r_1, r_2,... are the inner and outer radii of the annular voids.

Solving the two simultaneous equations, (28) and (29), these two equations become

$$J_o(\alpha \tilde{R}) Y_1(\alpha R_o) - Y_o(\alpha \tilde{R}) J_1(\alpha R_o) = 0 \qquad (31)$$

and similarly, for (28) and (30),

$$J_o(\alpha \tilde{R}) Y_1(\alpha \Delta R) - Y_o(\alpha \tilde{R}) J_1(\alpha \Delta R) = 0 \qquad (32)$$

Taking $\frac{R_o}{\tilde{R}} = \lambda_1$, $\frac{\Delta R}{\tilde{R}} = \lambda_2$, and $\alpha \tilde{R} = x$, (31) and (32) can be expressed as

$$J_o(x) Y_1(\lambda_1 x) - Y_o(x) J_1(\lambda_1 x) = 0 \qquad (33)$$

and

$$J_o(x) Y_1(\lambda_2 x) - Y_o(x) J_1(\lambda_2 x) = 0 \qquad (34)$$

This means that αR is equal to the value of x for which (33) or (34) is zero, dependent upon whether the effect of the central channel or the effect of an annular void is being analyzed. If λ is zero, or there are no voids in the system, the familiar re-

sult $\alpha R = 2.405$ is obtained.

The solution for $Z(z)$ yields

$$Z = C_2 \cos \beta z \tag{35}$$

and in order that $z = 0$ for $z = \tilde{H}/2$

$$\beta = \frac{\pi}{\tilde{H}}$$

therefore $B^2 = \alpha^2 + \beta^2$ or

$$B^2 = \left(\frac{x}{\tilde{R}}\right)^2 + \left(\frac{\pi}{\tilde{H}}\right)^2 \tag{36}$$

Since this is the geometrical buckling of the finite cylindrical reactor, it still must be equated to the material buckling obtained earlier, thus the new critical dimensions may be determined. The same arbitrary ratio of $\tilde{H}$ to $\tilde{D}$, i.e., $\tilde{H} = 2.2\,\tilde{R}$, is assumed for these calculations.

Numerical Analysis

Since the diameter of the "glory hole" has been established as 2.86 cm, or the radius as 1.44 cm, the ratio of $R_o/\tilde{R}$, where $\tilde{R}$ of the solid bare cylinder will be used as a first approximation, gives a value for $\lambda_1 = 1.43/10.04 = 0.143$. Thus (33) becomes

$$J_0(x)\,Y_1(0.143x) - Y_0(x)\,J_1(0.143x) = 0 \tag{37}$$

The value of x that satisfies (37) is 2.502, thus

$$B^2 = \left(\frac{2.502}{\tilde{R}}\right)^2 + \left(\frac{\pi}{\tilde{H}}\right)^2 \qquad (38)$$

or

$$\tilde{R}^2 = \frac{(2.502)^2}{B^2} + \frac{\pi^2}{4.14B^2} \qquad (39)$$

From this expression, the following values for $\tilde{R}$ and $\tilde{H}$ were determined.

$$\tilde{R} = 10.32 \text{ cm}$$

$$\tilde{H} = 22.70$$

Subtracting the extrapolation distance from these values, gives

$$R = 8.24 \text{ cm}$$

$$H = 18.54 \text{ cm}$$

The critical volume is thus

$$V_c = \pi R^2 H - \pi R_o^2 H$$

$$V_c = 3836.05 \text{ cm}$$

and the critical mass

$$M_c = 59.8 \text{ kg.}$$

Upon analysis of the annular voids, the change in the geometrical buckling was so minute, that the change in dimensions was so small that they were within the limits of error of the analytical

calculations. Consequently, the annular voids were assumed to have no appreciable effect on the critical dimensions of the system.

Dimension of the Shells

Several tests have been made relative to the tensile strength and mechanical properties of U-10 w/o Mo, and from these tests it has been established that a cylindrical shell of approximately 1/4 of an inch thick will maintain its structural integrity and stability throughout the range of temperatures under concern (Ref. 17). Thus, with this factor as a base, the pulse reactor under consideration can be divided into 10 cylindrical shells with a thickness of 0.65 cm, which is just slightly larger than the 1/4 in required.

Final Configuration

The final configuration, with the resultant critical dimensions, are as indicated in Figure 5. The critical mass for this configuration was computed to be 60.8 kg.

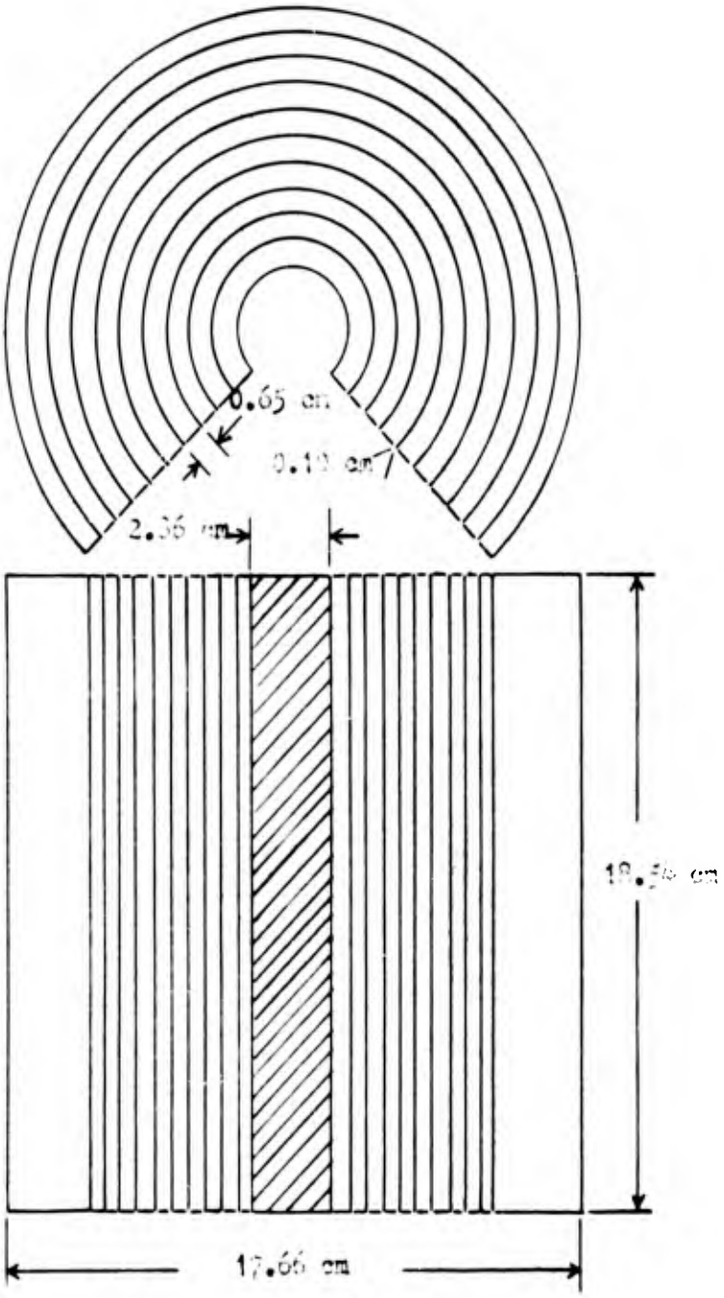

Figure 5

Cross-section of Pulse Facility Core

VI. Reactor Kinetics

Having found the critical size and mass of the pulse facility, it is now possible to study the neutronics of the system. To simplify the mathematics, the following discussions are based on the one group model. However, the values thus obtained for the various parameters should give fairly good approximations as to the orders of magnitude.

Steady State Flux Distribution

Since the flux has been assumed to be constant across the voids, the distribution in the core active material should closely approximate the distribution as given by

$$\phi = \phi_c J_o\left(\frac{2.502 r}{\hat{R}}\right)\cos\frac{\pi z}{\hat{H}} \tag{40}$$

where ϕ_c is the flux at the center line of the reactor, or in terms of the power

$$P = P_o J_o\left(\frac{2.502 r}{\hat{R}}\right)\cos\frac{\pi z}{\hat{H}} \tag{41}$$

The relative flux ϕ/ϕ_c was computed for various selected positions in the core and plotted in Figure 6.

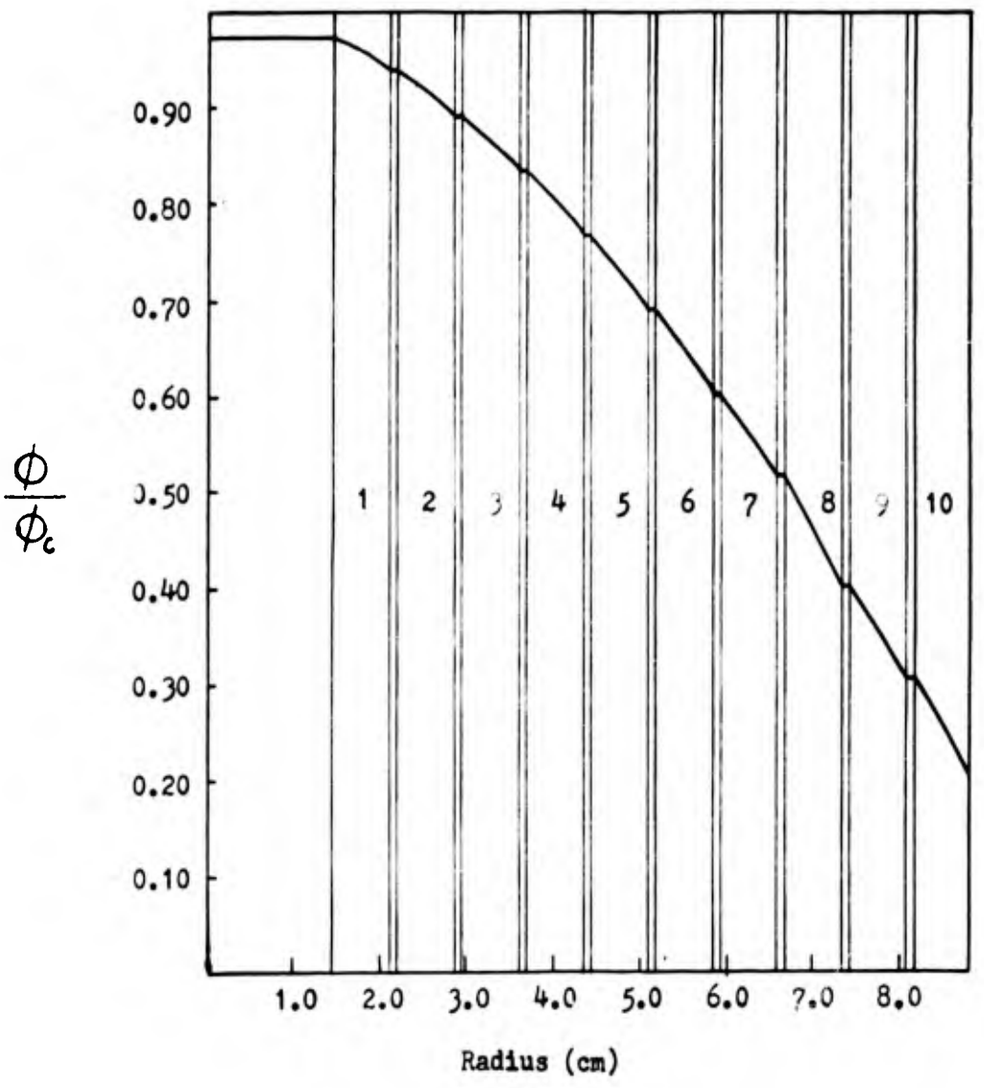

Figure 6

Steady State Flux Plot

Neutron Pulses

In this section, the characteristics of a controlled neutron burst is studied. The purpose of this study is to determine if the desired yield and surface leakage can be attained by pulsing the proposed reactor facility. In addition, some of the theory is developed which determines the pulse width, pulse width at half maximum, peak pulse, and other parameters associated with a pulsing cycle.

Because of the short pulse time in this facility, the pertinent features of the neutron burst may be closely approximated by an analysis based on prompt neutrons alone. The assumptions made in this analysis are as follows:

1. Delayed neutrons give no contribution
2. All reactor heat goes to raise the temperature
3. The number of neutrons is proportional to the power
4. Negative temperature coefficient

The one group reactor kinetics equation, neglecting delayed neutrons may be written as

$$\frac{dn}{dt} = \frac{\rho n}{\ell} \tag{42}$$

where n is the number of neutrons, ρ the excess reactivity over prompt critical, and ℓ the prompt neutron lifetime (Ref. 19). Since it has been postulated that the power is proportional to the

number of neutrons, (42) may also be written

$$\frac{dP}{dt} = \frac{\rho P}{\ell} \tag{43}$$

Excess Reactivity. With a negative temperature coefficient the excess reactivity over prompt critical is just

$$\rho = \rho_0 - \alpha T \tag{44}$$

where ρ_0 is the initial excess, α the temperature coefficient, and T the temperature. Equation (44) is an equation in three unknowns which is to be used as a basis for the solution of the transient equations involving the change in temperature as a result of the change in power.

Differentiating (44)

$$\dot{\rho} = -\alpha \dot{T}$$

$$\ddot{\rho} = -\alpha \ddot{T} \tag{45}$$

Now, since all the reactor heat goes to raise the temperature

$$\frac{dT}{dt} = \frac{P}{H} \tag{46}$$

where H is the total heat capacity of the core. Thus, substituting for $\dot{T}$,

$$\dot{\rho} = -\frac{\alpha P}{H} \tag{47}$$

and

$$\ddot{\rho} = -\frac{\alpha \dot{P}}{H} \tag{48}$$

Now dividing (48) by (47)

$$\frac{\ddot{\rho}}{\dot{\rho}} = \frac{\dot{P}}{P} \tag{49}$$

or substituting from (43)

$$\ddot{\rho} = \frac{\rho \dot{\rho}}{\ell} \tag{50}$$

Integrating, this becomes

$$\dot{\rho} = \frac{1}{2\ell}\rho^2 + C \tag{51}$$

If the time origin is chosen such that t = 0 at peak power P_m, where $\rho = 0$ and $\dot{\rho} = -\frac{\alpha P_m}{H}$, then

$$C = -\frac{\alpha P_m}{H}$$

and

$$\dot{\rho} = \frac{1}{2\ell}\rho^2 - \frac{\alpha P_m}{H} \tag{52}$$

or, letting $\beta^2 = 2\ell \alpha P_m / H$

$$\frac{2\ell\, d\rho}{\beta^2 - \rho^2} = -dt \tag{53}$$

integrating again

$$\frac{2\ell}{\beta}\,\mathrm{Tanh}^{-1}\frac{\rho}{\beta} = -t + C_1 \tag{54}$$

since $\rho = 0$ at $t = 0$, $c_1 = 0$, hence

$$\rho = -\beta\,\mathrm{Tanh}\left(\frac{\beta t}{2\ell}\right) \tag{55}$$

Peak Pulse. Now, returning to the basic equations and dividing (43) by (46)

$$\frac{dP}{dt} = \frac{\rho H}{\ell}\frac{dT}{dt} = \frac{(\rho_o - \alpha T)H}{\ell}\frac{dT}{dt} \tag{56}$$

or,

$$\frac{dP}{dT} = \frac{(\rho_o - \alpha T)H}{\ell}$$

and then integrating,

$$P = \frac{H}{\ell}\left(\rho_o T - \frac{\alpha T^2}{2}\right) + P_o \tag{57}$$

assuming that $P_m >> P_o$, at P_m, $T = \rho_o/\alpha$

Thus,

$$P_m = \frac{H}{\ell}\left(\frac{\rho_o^2}{\alpha} - \frac{\alpha\rho_o^2}{2\alpha^2}\right) \tag{58}$$

rearranging,

$$P_m = \frac{\rho_o^2 H}{2\alpha\ell} \tag{59}$$

Equation (59) gives the expression for the peak power in the system. If (59) is rearranged, it can be seen that ρ_o is just equal to β, thus

$$\rho = -\rho_o \, Tanh\left(\frac{\rho_o t}{2\ell}\right) \tag{60}$$

which gives the excess activity remaining at any time t.

Power During Pulse. Differentiating (60),

$$\dot{\rho} = \frac{\rho_o^2}{2\ell} sech^2\left(\frac{\rho_o t}{2\ell}\right) \tag{61}$$

and substituting into (47), substituting for ρ_o^2 from (59), and rearranging gives

$$P = P_m sech^2\left(\frac{\rho_o t}{2\ell}\right) \tag{62}$$

which is the power at any time t.

Pulse Width. In order to determine the pulse width at half maximum, set

$$\frac{P}{P_m} = sech^2\left(\frac{\rho_o t_i}{2\ell}\right) = \frac{1}{2} \tag{63}$$

$$\operatorname{sech}\left(\frac{\rho_o t_{\frac{1}{2}}}{2\ell}\right) = \frac{1}{\sqrt{2}}$$

$$\cosh\left(\frac{\rho_o t_{\frac{1}{2}}}{2\ell}\right) = \sqrt{2}$$

$$\frac{\rho_o t_{\frac{1}{2}}}{2\ell} = 0.88138$$

$$t_{\frac{1}{2}} = 1.76276\,\frac{\ell}{\rho_o} = 1.76276\,\tau \tag{64}$$

where $\tau = \ell/\rho_o$ is just the initial period of the reactor. However, since $2\,t_{\frac{1}{2}} = \Delta t =$ the pulse width,

$$\Delta t = 3.52552\,\tau \tag{65}$$

Total Energy. The total energy expended w_α in the pulse may be determined by rearranging (47) and integrating from zero to infinity, i.e.,

$$w_\alpha = \int_0^\alpha P\,dt = -\frac{H}{\alpha}\int_0^\alpha \dot{\rho}\,dt = -\frac{H}{\alpha}\int_\circ^{-\rho_o} d\rho \tag{66}$$

thus, $w_\alpha = 2H\rho_o/\alpha$ (67)

Since it has been assumed that $T = \rho/\alpha$ at P_m, then the average temperature rise would be $\Delta T/2$ which is approximately T, hence $\Delta T = 2\rho_o/\alpha$. Consequently, from (67)

$$w_\alpha = H\,\Delta T \tag{68}$$

Numerical Evaluation. In order to evaluate the performance of the pulse facility, it is necessary to find numerical values for some of the parameters derived in the previous section. It has been established, based on the melting point of the U-10 w/o Mo alloy, that the maximum temperature rise should be limited to 800° C. Therefore, this value will be used to first determine the total energy expended. Thus, from (68),

$$W_{\alpha} = H\Delta T = M_c c_p \Delta T \tag{69}$$

where c_p is the specific heat of the core material and M_c is the critical mass as defined previously. There is one problem involved in the above expression and that is that c_p is also a function of the temperature. However, a temperature interval average may be used that will give fairly good results. These values, plus their temperature intervals, and the total energy for each interval are shown in Table VII.

If it is assumed that the pulse reactor has a fission yield for the assembly similar to that of Godiva II, the total yield per pulse may also be determined. In Godiva II, each fission yields 178 Mev to the assembly with a 1.2 correction to center. In addition, the measured leakage from the Godiva II assembly has been determined to be 1.4 leakage neutrons for each fission (Ref. 33). These values are rather conservative for the pulse reactor, however,

Table VII

Total Energy Expended in Pulse

M_c = 60 kg = 6.0×10^4 gm

T(°C)	c_p(cal/gm° C)*	Energy (Mev)
20-200	0.0310	0.88×10^{19}
200-400	0.0333	1.05×10^{19}
400-600	0.0383	1.20×10^{19}
600-800	0.0460	1.44×10^{19}
	Total Energy Expended	4.57×10^{19} Mev

* Reference 2

they should be representative of the order of magnitudes. The total yield Y becomes

$$Y = \frac{W_{oc}(Mev)}{1.2\left(178 \frac{Mev}{fission}\right)} = \frac{4.57 \times 10^{19}}{213.6} = 2.14 \times 10^{17} \text{ fissions}$$

Consequently, the leakage L would be

$$L = 2.14 \times 10^{17} \text{ fissions} \times 1.4 \frac{\text{leakage neutrons}}{\text{fission}}$$

$$L = 3.00 \times 10^{17} \text{ neutrons}$$

The surface leakage can be determined by dividing the total leakage above by the surface area of the pulse facility. The sur-

face area is approximately 1800 cm^2 , thus the surface leakage would be about 1.67×10^{14} neutrons/cm^2.

Other representative values from Godiva II may also be chosen, such as the negative temperature coefficient of 0.4/°C, and other parameters of interest may be obtained from the expressions derived in the previous section. For example, if (67) is divided by (59),

$$\frac{W_{ac}}{P_m} = \frac{2H\rho_0}{\alpha} \cdot \frac{2l\alpha}{\rho_0^2 H} = \frac{4l}{\rho_0} = 4\gamma = \frac{4\Delta t}{3.53} \qquad (70)$$

or $P_m = \frac{0.88\, W_{ac}}{\Delta t}$

if $\Delta t = 10\,\mu$ sec, then

$$P_m = \frac{(0.88)(4.57 \times 10^{19})}{10^{-5} \text{ sec}} = 4.0 \times 10^{24} \frac{\text{Mev}}{\text{sec}}$$

$$P_m = 6.45 \times 10^5 \text{ megawatts}$$

VII. Discussion of Results

The analysis of a pulse reactor is extremely difficult following established hand calculational procedures. The calculations are very long and tedious and errors are easily made. Consequently, it is necessary to check and recheck every step as it is taken. In addition, there are other pertinent features of the pulse facility that should be studied that is impossible to analyze by hand calculations. Therefore, it is heartily recommended that computers be used in this type of analysis. However, it is felt that this discussion has given fairly representative values for this type of facility.

Experimental assembly of a critical facility is the only really accurate method for the determination of the critical mass of a given material. Therefore, the value obtained, in this report, of 60 kg is just an approximation. However, it should be a fairly good approximation. The "Hachet Code" has been used in a computer analysis of a system that is very similar to the one under discussion. In this analysis, the critical mass was estimated at 62.7 kg (Ref. 1). Thus, a value of 60 kg is within the limits of error of both analytical methods.

Although the total yield of the pulse facility was computed based on characteristics of the Godiva II reactor, the value ob-

tained should be representative of the order of magnitude and should also be rather conservative. Thus, the design requirement of approximately 10^{17} neutrons per pulse appears to be attained since the computed value was 2.14×10^{17} neutrons/pulse.

An analysis of the percentage of leakage neutrons leaving the reactor in the axial direction and radial direction was attempted, based on the isotropic motion of the neutrons and the geometry of the system, but this was found to be impossible to accomplish in a hand calculation. In each annular void there are five probabilities, each of which is dependent upon the other. The probabilities are:

1. A neutron leaving an inner region enters an outer region.
2. A neutron leaving the inner region escapes vertically out of the void.
3. A neutron leaving an outer region enters an inner region.
4. A neutron leaving an outer region re-enters the outer region.
5. A neutron leaving an outer region escapes vertically out of the void.

For a single void, these probabilities are not too difficult to establish. However, since the radius of curvature is different

for each void, the five probabilities established for each void would also be different. Thus, with a total of 10 voids, there would be a sum total of fifty probabilities. To sum these probabilities up over the inner surface and the outer surface of each void involves thousands of equations and calculations. Consequently, these percentages would have to be determined experimentally or by a computer analysis.

The total leakage, however, should be larger than that of Godiva II and, since Godiva's leakage spectrum approximates the fission spectrum (see Fig. 2), it is postulated that the leakage spectrum of the pulse assembly will also be similar to the fission spectrum. The computed value for the total leakage from the pulse facility was 3.0×10^{17} n/pulse.

The over-all results of this analysis appear to indicate that the general design requirements for a pulse facility would be attained by this particular configuration and material. Uranium-molybdenum alloys give the necessary stability and physical integrity to the core to withstand the high temperatures involved and the configuration reduces the mechanical stresses.

In terms of economy, the critical mass of the proposed pulse facility is just slightly larger than that of Godiva II, with much improved performance characteristics. In addition, the cylindrical shells are particularly adaptable for almost any type of fabrication.

A summary of a few of the performance characteristics of the proposed pulse facility and Godiva II is shown in Table VIII for comparison purposes.

Table VIII

Performance of Proposed Pulse Facility
as Compared to Godiva II

	Proposed System	Godiva*
Maximum Temperature Rise (^{o}C)	800	100
Total Energy/pulse (megawatt-sec)	6.90	0.433
Pulse Width (μ sec)	10	80
Peak Power (megawatts)	6.45×10^{5}	3.23×10^{3}
Total Yield (n/pulse)	2.14×10^{17}	1.4×10^{16}
Surface Leakage (n/cm^{2}/pulse)	1.67×10^{14}	9.32×10^{12}

* Reference 34

VIII. Conclusion

There are several analytical methods available that are suitable for hand calculations involving the determination of the critical mass of a reactor. However, the most accurate, for a fast reactor appears to be the Multigroup Asymptotic Transport Method. This method gives a value for the material buckling of a system to which the geometric buckling must be equated in order to attain a critical configuration. Consequently, once a fuel material has been selected, it is possible to determine the physical dimensions for almost any configuration.

In the analysis of the voids, they were treated as if they were vacuums. However, there are several gas coolants that have very small cross sections for interaction which simulate a vacuum very closely. Consequently, if a gas such as helium is used to cool the reactor, the analysis can be assumed to be valid.

The values obtained for the total energy expended in a pulse, the leakage, surface leakage, etc., were all primarily based on the assumption that the delayed neutrons had no effect on the characteristics of a pulse. In addition, it was also assumed that some of the features of Godiva II was applicable to this system. Although these assumptions are not strictly true, the values obtained using these assumptions should be fairly representative of the orders

of magnitude.

Recommendations

To carry this analysis further, it is recommended that a study should be made as to the temperature distribution in the core. A knowledge of the temperature distribution would permit a better optimization of the dimensions of the voids and also the fuel shells. In addition, the amount of heat that should be removed from the system by the coolant to maintain the proper temperature ranges would also be derived from this study. These facts, in turn, would give information relative to the type of coolant to use, the mass flow required, and the pumping power necessary to attain the mass flow.

Another area that should be investigated, is the stresses involved in the system as a result of a pulse. However, these are rather difficult to analyze and a computer should be used if possible.

Possible methods for pulsing the system by the introduction of excess reactivity, should also provide a more complete analysis in future investigations.

The most significant area that should be considered for subsequent examinations into the proposed facility involves the safety aspects of operation. For example, how high of an excursion can the proposed facility withstand before a meltdown occurs, or what

are the hazards to be considered upon a complete closure of the voids. There are also other safety factors that should be theoretically analyzed prior to the time of any attempt at operation.

These additional investigations, added to the information contained in this report, should provide a complete analysis of a pulse reactor of this configuration. In fact, it should provide enough information to safely start, and complete, a critical, slow-assembly experiment.

Bibliography

1. Bohannon, J.R. Private Communication, Institute of Technology (AU), (Jan. 1961).

2. Boyle, R.F. "Calorimetric Determination of Ordering in the U-Mo System," WAPD, PWR, PMM, 633, (1956).

3. Calkins, G.D. "Effects of Heat Treatment and Burn-up on Radiation Stability of 10% by Weight Molybdenum-Uranium Fuel Alloys," ASTM Special Technical Publication, No. 220, (1958).

4. Calkins, G.D. "Radiation Stability Studies on Binary Uranium Alloys," POTSNESC, Vol. II, Part II, pp 272-281, (1957).

5. Chernick, J. & Kaplan, I. "The Nuclear Reactor with a Transverse Air Gap," J. Nuclear Energy, Vol. 2, pp 41-51, (1955).

6. Critoph, E. & Pearce, R.M. "The Reactivity Effect Due to Neutron Streaming in an Empty Tube," J. Nuclear Energy, Vol. 4, pp 445-459, (1957).

7. Del Grosso, A. "Compilation of Uranium 10 w/o Molybdenum Fuels Alloy Properties," APDA Technical Memorandum No. 3, (June 1957).

8. "Enrico Fermi Atomic Power Plant," APDA 124, (Jan. 1959).

9. Etherington, H., (ed). Nuclear Engineering Handbook, McGraw-Hill Book Co., N.Y., N.Y., (1958).

10. Fuchs, K. Efficiency for Very Slow Assembly, LA-596, (1946).

11. Fuchs, K. "Perturbation Theory in Neutron Multiplication Problems," Proceedings of the Royal Physical Society, Vol. 62A London, (1949).

12. Gamba, O., et al. "Natural Uranium-Beryllium and Natural Uranium Oxides-Metallic Beryllium Lattices: Computation of Cylindric Reactors," Proceedings of the International Conference on the Peaceful Uses of Atomic Energy, Geneva, (1955).

13. Glasstone, S. and Edlund, M.C. The Elements of Nuclear Reactor Theory, D. Van Nostrand Co., p 64, (1952).

14. Glasstone, S. (ed). The Effects of Nuclear Weapons, United States Atomic Energy Commission, Washington, D.C., (1957).

15. Kopelman, B. Materials for Nuclear Reactors, McGraw-Hill, N.Y., (1959).

16. Mandl, M.E. Calculation of the Thermal Fine Structure in a Pile with Hollow Rods by the Spherical Harmonics Method, AERE T/M-46, Harwell, Berks, England, (1956).

17. "Mechanical Properties of Uranium-Molybdenum Alloys," United Kingdom Atomic Energy Authority, AERE M/R 2554, (1958).

18. Metchell, H.M. "Concentric Voids in Spherical Reactors and Cells," Masters Thesis, North Carolina State College, N.C., (1960).

19. Murray, R.L. Nuclear Reactor Physics, Prentice-Hall, Inc., Englewood Cliffs, N.J., (1957).

20. Newmarch, D.A. "A Modification to the Diffusion Theory of the Thermal Fine Structure in a Reactor to Account for the Effects of Air Channels," J. Nuclear Energy, Vol. 2, pp 52-58, (1955).

21. Okrent, D. On the Application of Multigroup Diffusion Theory to Fast Critical Assemblies, Report, ANL-5321, (1954).

22. Patry, J. and Meier, R.W. "Influence on Reactivity of an Air Gap between Two Concentric Regions of a Cylindrical Reactor." Proceedings of the Second International Conference on the Peaceful Uses of Atomic Energy, Geneva, Vol. 13, pp 111-116, (1958).

23. Paxton, H.C. "Critical Assemblies at Los Alamos," Nucleonics, Vol. 13, No. 10, p 48 (1955).

24. Price, W.J. Nuclear Radiation Detection, McGraw-Hill Book Co., N.Y., (1958).

25. Reactor Physics Constants, ANL-5800, p 48 (1955).

26. Stephenson, R. Introduction to Nuclear Engineering, McGraw-Hill Book Co., Inc., N.Y., (1958).

27. Stratton, W.R., et al. "Analysis of Prompt Excursions in Simple Systems and Idealized Fast Reactors," Proceedings of the Second International Conference on the Peaceful Uses of Atomic Energy, Geneva, Paper 431, (1958).

28. Stummel, F. "On the Theory of Cylindrical Air Gaps in Nuclear Reactors," Proceedings of the Second International Conference on the Peaceful Uses of Atomic Energy, Geneva, Vol. 13, pp 105-110, (1958).

29. Tait, J.H. "The Calculation of the Fine Structure of the Thermal Neutron Flux in a Pile by the Spherical Harmonics Method," Proceedings of the International Conference on the Peaceful Uses of Atomic Energy, Geneva, Vol. 5, pp 417-422, (1955).

30. Tipton, C.R. (ed). Reactor Handbook: Materials, Vol. I, pp 148-204, Interscience Publishers, Inc., N.Y., (1960).

31. Weinberg and Wigner. The Physical Theory of Neutron Chain Reactors, The University of Chicago Press, Chicago 37, (1958).

32. Wimett, T.F. Time Behavior of Godiva Through Prompt Critical, LA-2029, (1956).

33. Wimett, T.F. and Orndoff J.D. Applications of Godiva II Neutron Pulses, Report 419, (June 1958).

34. Zipprich, L.J. Radiation Effects Testing at the Los Alamos Godiva II Facility, Sandia Corporation Reprint, TID-4500, (April 1959).

Appendix A

List of Symbols

A = constant

α = coefficient of thermal expansion

α = temperature coefficient

α = constant

B = square root of buckling

B^2 = material and geometric buckling

β = constant

C = constant

D_j = diffusion coefficient for group j

E_L = lowest energy level for any group

$F(r)$ = spatial shape factor

γ_j = fraction of neutrons born in group j

$\tilde{H}$ = extrapolated height of reactor

H = physical height of reactor

H = total heat capacity of reactor

J_o = Bessel function of first kind

ℓ = prompt neutron lifetime

L = total reactor leakage

M_c = critical mass

n = neutron density

N = atoms / cm^3

ν = neutrons born / fission

P = reactor power

P_m = peak power

P_o = initial power

$\tilde{R}$ = extrapolated radius of reactor

R = physical radius of reactor

ρ = excess reactivity above prompt critical

ρ_o = initial excess reactivity

S_j = source term

σ_c = microscopic capture cross section

σ_{er} = microscopic elastic removal cross section

σ_f = microscopic fission cross section

σ_{in} = microscopic inelastic scatter cross section

σ_{tr} = transport cross section

Σ_c = macroscopic capture cross section

Σ_{el-mod} = macroscopic elastic moderation cross section

Σ_{el-tr} = macroscopic elastic transport cross section

Σ_f = macroscopic fission cross section

Σ_{in} = macroscopic inelastic scattering cross section

$\Sigma_{removal}$ = total removal macroscopic cross section

Σ_{tr} = macroscopic transport cross section

t = time

T = temperature

r = reactor period

ϕ = neutron flux

ϕ_c = centerline neutron flux

V_c = critical volume

W_{tot} = total energy

Y_o = Bessel function of second kind

Y = total yield

Appendix B

Sample Calculations

Multigroup Asymptotic Transport Iteration

First iteration:

$$\phi_j = \frac{\gamma_j \sum_{k=1}^{N} \nu_k \Sigma_{f,k} \phi_k + \sum_{\ell=1}^{j-1} \Sigma_{in}(\ell \to j)\phi_\ell + \sum_{m=1}^{j-1} \Sigma_{er}(m \to j)\phi_m}{\frac{B}{\tan^{-1}\frac{B}{\Sigma_{tr,j}}} - \Sigma_{el-tr,j}}$$

Assume

$$\sum_{k=1}^{N} \nu_k \Sigma_{f,k} \phi_k = 1$$

Then

$$\phi_j = \frac{\gamma_j + \sum_{\ell=1}^{j-1} \Sigma_{in}(\ell \to j)\phi_\ell + \sum_{m=1}^{j-1} \Sigma_{er}(m \to j)\phi_m}{\frac{B}{\tan^{-1}\frac{B}{\Sigma_{tr,j}}} - \Sigma_{el-tr,j}}$$

Try B = 0.2885

$$\phi_1 = \frac{\gamma_1}{\frac{B}{\text{Tan}^{-1}\frac{B}{\Sigma_{tr,1}}} - \Sigma_{el-tr,1}}$$

From Tables II and V

$$\gamma_1 = 0.338$$

$$\Sigma_{tr,1} = 0.20541$$

$$\Sigma_{el-tr,1} = 0.05083$$

$$\frac{B}{\Sigma_{tr,1}} = \frac{0.2885}{0.20541} = 1.4045$$

$$\text{Tan}^{-1}\frac{B}{\Sigma_{tr,1}} = \text{Tan}^{-1}(1.4045) = 0.95237$$

$$\frac{B}{\text{Tan}^{-1}\frac{B}{\Sigma_{tr,1}}} = \frac{0.2885}{0.95237} = 0.30293$$

$$\frac{B}{\text{Tan}^{-1}\frac{B}{\Sigma_{tr,1}}} - \Sigma_{el-tr,1} = 0.30293 - 0.05083 = 0.25210$$

Following the same procedure:

$$\phi_4 = 1.10637$$

$$\phi_5 = 0.87536$$

$$\phi_6 = 0.87832$$

$$\phi_7 = 0.38881$$

$$\phi_8 = 0.16406$$

$$\phi_9 = 0.10140$$

$$\phi_{10} = 0.02818$$

$$\phi_{11} = 0.00157$$

To check for convergence:

$$\nu_1 \Sigma_{f,1} \phi_1 = (0.13849)(1.34074) = 0.18568$$

$$\nu_2 \Sigma_{f,2} \phi_2 = (0.12963)(1.23790) = 0.16047$$

$$\vdots \qquad \vdots \qquad \vdots$$

$$\nu_{11} \Sigma_{f,11} \phi_{11} = (0.55382)(0.00157) = \underline{0.00087}$$

$$\sum_{N=1}^{N} \nu_N \Sigma_{f,N} \phi_N = 0.97612$$

Does not converge to enough accuracy, start second iteration.

Appendix C

Godiva Verification

N_1(U-235) = 0.04498 x 10^{24} atoms/cm^3

N_2(U-238) = 0.00302 x 10^{24} atoms/cm^3

B = 0.290

J	S_j^*	$\sum_{in(1\to j)}\phi_1$	$\sum_{in(2\to j)}\phi_2$	$\sum_{in(3\to j)}\phi_3$	j
1	0.338	-	-	-	1
2	0.236	0.05306	-	-	2
3	0.178	0.03850	0.04605	-	3
4	0.116	0.02375	0.02845	0.03263	4
5	0.066	0.01299	0.01647	0.01790	5
6	0.033	0.00685	0.00804	0.00990	6
7	0.017	0.00374	0.00404	0.00495	7
8	0.008	0	0.00239	0.00227	8
9	0.006	0	0	0.00168	9
10	0.002	0	0	0	10
11	0	0	0	0	11

$$\phi_1 = \frac{0.338}{0.25210} = 1.34074$$

$$\phi_2 = \frac{\gamma_2 + \sum_{in}(1\to 2)\phi_1 + \sum_{ex}(1\to 2)\phi_1}{\frac{B}{\tan^{-1}\frac{B}{\Sigma_{tr,2}}} - \sum_{el-tr,2}}$$

In the same manner as before:

$$\frac{B}{\tan^{-1}\frac{B}{\Sigma_{tr,2}}} - \sum_{el-tr,2} = 0.23346$$

$$\phi_2 = \frac{0.236 + 0.05248 + 0.00052}{0.23346}$$

$$\phi_2 = 1.23790$$

$$\phi_3 = \frac{\gamma_3 + \sum_{in}(1\to 3)\phi_1 + \sum_{in}(2\to 3)\phi_2 + \sum_{ex}(2\to 3)\phi_2}{\frac{B}{\tan^{-1}\frac{B}{\Sigma_{tr,3}}} - \sum_{el-tr,3}}$$

$$\phi_3 = \frac{0.178 + 0.04007 + 0.04620 + 0.00097}{0.19329}$$

$$\phi_3 = 1.37224$$

j	$\sum_{in}(4\to j)\phi_4$	$\sum_{in}(5\to j)\phi_5$	$\sum_{in}(6\to j)\phi_6$	$\sum_{in}(7\to j)\phi_7$	j
1	-	-	-	-	1
2	-	-	-	-	2
3	-	-	-	-	3
4	-	-	-	-	4
5	0.02675	-	-	-	5
6	0.01386	0.01360	-	-	6
7	0.00693	0.00622	0.00563	-	7
8	0.00353	0.00319	0.00256	0.00056	8
9	0.00257	0.00231	0.00179	0	9
10	0.00064	0.00055	0.00042	0	10
11	0	0.00016	0.00012	0	11

j	$\sum_{in}(8\to j)\phi_8$	$\sum_{in}(9\to j)\phi_9$	$\sum_{in}(10\to j)\phi_{10}$	$\sum_{el\text{-}mod}(j\to j+1)$	j
1	-	-	-	0.00052	1
2	-	-	-	0.00099	2
3	-	-	-	0.00218	3
4	-	-	-	0.00190	4
5	-	-	-	0.00247	5
6	-	-	-	0.00236	6
7	-	-	-	0.00198	7
8	-	-	-	0.00095	8
9	0.00017	-	-	0.00028	9
10	0.000009	0.000008	-	0.00005	10
11	0	0.000005	0	-	11

j	$S_j + \sum_{\ell=1}^{j-1} \Sigma_{in}(\ell-j)\phi_\ell$ *	$\Sigma_{el-tr,j}$	$\Sigma_{tr,j}$	$B/\Sigma_{tr,j}$	j
1	0.33800	0.03922	0.21660	1.33890	1
2	0.28958	0.06087	0.21600	1.34260	2
3	0.26354	0.11261	0.23100	1.25540	3
4	0.20301	0.12764	0.24601	1.17880	4
5	0.14201	0.20067	0.30360	0.95520	5
6	0.08772	0.28135	0.38026	0.76264	6
7	0.05087	0.36827	0.46320	0.62608	7
8	0.02443	0.40728	0.52320	0.55428	8
9	0.01547	0.44835	0.58801	0.49319	9
10	0.00391	0.43601	0.64800	0.44753	10
11	0.00034	0.30075	0.68640	0.42249	11

* $\sum_{\ell=1}^{j-1} \Sigma_{in}(\ell-j)$ includes $\Sigma_{er}(\ell \to j)$

j	$\tan^{-1} B/\Sigma_{tr,j}$	$B/\tan^{-1}(B/\Sigma_{tr,j})$	$[B/\tan^{-1}(B/\Sigma_{tr,j})] - \Sigma_{el-tr}$	ϕ_j	j
1	0.92928	0.31207	0.27285	1.23878	1
2	0.93060	0.31163	0.25076	1.15481	2
3	0.89812	0.32290	0.21029	1.25322	3
4	0.86726	0.33439	0.20675	0.98191	4
5	0.76247	0.38034	0.17967	0.79039	5
6	0.65153	0.44511	0.16376	0.53566	6
7	0.55937	0.51844	0.15017	0.33875	7
8	0.50611	0.57300	0.16572	0.14772	8
9	0.45818	0.63294	0.18459	0.08381	9
10	0.42080	0.68916	0.25315	0.01543	10
11	0.39974	0.72547	0.42472	0.00079	11

$\sum S_j = 1000$

$\sum_{k=1}^{11} \nu_k \Sigma_{f,k} \phi_k = 1.0210$ converges

$$B = 0.290$$

$$B^2 = 0.084$$

$$B^2 = \frac{\pi^2}{\tilde{R}^2} \quad \text{(For Godiva I)}$$

$$\tilde{R}^2 = \frac{\pi^2}{B^2} = \frac{9.8696}{0.084} = 117.5$$

$$\tilde{R} = 10.83 \text{ cm}$$

Extrapolation distance from ANL-5800

$$d = 2.08 \text{ cm}$$

$$R = 10.83 - 2.08 = 8.75 \text{ cm}$$

Density of Godiva composition

$$\rho = 18.75 \text{ gms/cm}^3$$

$$M_c = \frac{4}{3}\pi R^3 \rho = (4.188)(8.75)^3(18.75)$$

$$M_c = (4.188)(669.9)(18.75)$$

$$M_c = 52.6 \text{ kg}$$

$$M_c(\text{Godiva}) = 52 \text{ kg}$$

GNE/Phys/61-11

Vita

James [redacted] Mann was [redacted] he entered the U.S. Army Air Force and, after completing flight training, flew 35 combat missions over Europe during World War II. Upon his separation in September 1945, he enrolled in the University of Louisville and majored in Physics and Mathematics. He was graduated in June 1950 with the degree of Bachelor of Arts and immediately enrolled in the University of Kentucky for graduate work. However, prior to the completion of this work, the U.S. Air Force, in April 1951, recalled him to active duty. He flew 37 combat missions over Korea and then was assigned as instructor pilot with the Strategic Air Command. His last assignment prior to his coming to the Institute of Technology was as instructor pilot in the B-47, also for the Strategic Air Command.

Permanent Address: [redacted]

This thesis was typed by Mrs. J.H. Mann

UNCLASSIFIED